
Article:
Aad, G. orcid.org/0000-0002-6665-4934, Abbott, B. orcid.org/0000-0002-5888-2734, Abbott, D.C. orcid.org/0000-0002-7248-3203 et al. (2895 more authors) (2023) Correlations between flow and transverse momentum in Xe + Xe and Pb + Pb collisions at the LHC with the ATLAS detector: a probe of the heavy-ion initial state and nuclear deformation. Physical Review C, 107 (5). 054910. ISSN 2469-9985

https://doi.org/10.1103/physrevc.107.054910

Correlations between flow and transverse momentum in Xe + Xe and Pb + Pb collisions at the LHC with the ATLAS detector: A probe of the heavy-ion initial state and nuclear deformation

G. Aad *et al.*[*]
(ATLAS Collaboration)

(Received 3 May 2022; accepted 29 August 2022; published 15 May 2023)

The correlations between flow harmonics v_n for $n = 2$, 3, and 4 and mean transverse momentum $[p_T]$ in $^{129}Xe + {}^{129}Xe$ and $^{208}Pb + {}^{208}Pb$ collisions at $\sqrt{s} = 5.44$ and 5.02 TeV, respectively, are measured using charged particles with the ATLAS detector. The correlations are potentially sensitive to the shape and size of the initial geometry, nuclear deformation, and initial momentum anisotropy. The effects from nonflow and centrality fluctuations are minimized, respectively, via a subevent cumulant method and an event-activity selection based on particle production at very forward rapidity. The v_n-$[p_T]$ correlations show strong dependencies on centrality, harmonic number n, p_T, and pseudorapidity range. Current models qualitatively describe the overall centrality- and system-dependent trends but fail to quantitatively reproduce all features of the data. In central collisions, where models generally show good agreement, the v_2-$[p_T]$ correlations are sensitive to the triaxiality of the quadruple deformation. Comparison of the model with the Pb + Pb and Xe + Xe data confirms that the ^{129}Xe nucleus is a highly deformed triaxial ellipsoid that has neither a prolate nor oblate shape. This provides strong evidence for a triaxial deformation of the ^{129}Xe nucleus from high-energy heavy-ion collisions.

DOI: 10.1103/PhysRevC.107.054910

I. INTRODUCTION

Heavy-ion collisions at the Relativistic Heavy Ion Collider (RHIC) and the Large Hadron Collider (LHC) produce quark-gluon plasma (QGP), whose space-time evolution is well described by relativistic viscous hydrodynamics [1–3]. Driven by the large pressure gradients, the QGP expands rapidly in the transverse plane, and converts the spatial anisotropy in the initial state into momentum anisotropy in the final state. The collective expansion in each event is quantified by Fourier expansions of particle distributions in azimuth given by $dN/d\phi = (N/2\pi)[1 + 2\sum_{n=1}^{\infty} v_n \cos n(\phi - \Psi_n)]$, where v_n and Ψ_n represent the amplitude and phase of the nth-order azimuthal flow vector, $\boldsymbol{V}_n = v_n e^{in\Psi_n}$. The $\boldsymbol{V}_n$ are determined by the hydrodynamic response to the initial spatial anisotropy, characterized by eccentricity vectors $\mathcal{E}_n = \varepsilon_n e^{in\Phi_n}$ [4,5]. Model calculations show that the $\boldsymbol{V}_n$ values are approximately proportional to $\mathcal{E}_n$ for $n = 2$ and 3, as well as for $n = 4$ in central collisions [4,6,7]. The measurements of v_n and Ψ_n [8–14] have placed important constraints on the properties of the medium and on the initial-state density fluctuations [5–7,15–17] in high-energy nuclear collisions.

In addition to generating anisotropic flow, the hydrodynamic response to the fluctuations in the overall size of the overlap region also leads to fluctuations in the "radial flow," reflected by the average transverse momentum of particles in each event, $[p_T]$.[1] In particular, events with similar total energy but smaller transverse size in the initial state are expected to have a stronger radial expansion and therefore a larger $[p_T]$ [18,19]. Furthermore, correlations between the $\mathcal{E}_n$ and the size in the initial state are expected to generate dynamical correlations between v_n and $[p_T]$ in the final state. A Pearson coefficient has been proposed to study these correlations [20],

$$\rho_n = \frac{\langle\langle v_n^2 \delta p_T \rangle\rangle}{\sqrt{\left(\langle v_n^4 \rangle - \langle v_n^2 \rangle^2\right)} \sqrt{\langle\langle \delta p_T \delta p_T \rangle\rangle}}, \tag{1}$$

where $\delta p_T = p_T - [p_T]$, the "$\langle\langle\ \rangle\rangle$" denotes averaging over all particle pairs or triplets for events with comparable particle multiplicity, and the "$\langle\ \rangle$" denotes an averaging over events. Due to centrality dependence of collision geometry and nucleon fluctuations, the ρ_n is expected to be positive in central and mid-central collisions and negative in the peripheral collisions [21]. In the presence of initial momentum anisotropy, the ρ_n could turn into positive in the most peripheral region [22]. The root-mean-square size of the nucleon also influences the behavior of ρ_n in peripheral collisions,

[*]Full author list given at the end of the article.

[1]ATLAS uses a right-handed coordinate system with its origin at the nominal interaction point (IP) in the center of the detector and the z axis along the beam pipe. The x axis points from the IP to the center of the LHC ring, and the y axis points upward. Cylindrical coordinates (r, ϕ) are used in the transverse plane, ϕ being the azimuthal angle around the beam pipe. The pseudorapidity is defined in terms of the polar angle θ as $\eta = -\ln\tan(\theta/2)$.

e.g., a larger nucleon size would decrease the value of ρ_n [23]. ATLAS published a measurement of ρ_n for $n = 2$, 3, and 4 in Pb + Pb collisions at $\sqrt{s_{NN}} = 5.02$ TeV [24], which was followed by a similar measurement from ALICE [25] in Pb + Pb and Xe + Xe collisions. The results show positive correlations for all harmonics, except in the peripheral region, where ρ_2 is negative. These behaviors have been qualitatively reproduced by recent initial-state model and hydrodynamic model calculations [21,26].

Recent studies show that the v_n, $[p_T]$, and v_n-$[p_T]$ correlations in central collisions are also sensitive to the shape of atomic nuclei [27–32]. Most nuclei are more or less deformed into an ellipsoidal shape, for which the nuclear surface of the nucleon distribution can be described by [33]

$$R(\theta, \phi) = R_0(1 + \beta[\cos\gamma Y_{2,0} + \sin\gamma Y_{2,2}]), \qquad (2)$$

where R_0 is the nuclear radius, $Y_{l,m}$ are spherical harmonics, and β and γ are quadrupole deformation parameters. The parameter β is the magnitude of the deformation, with typical values of 0.1–0.4 [34], while the angle γ, in the range $0 \leqslant \gamma \leqslant 60^\circ$, describes the length imbalance of the three semiaxes r_1, r_2, r_3 of the ellipsoid, also known as triaxiality. The values $\gamma = 0^\circ$, $\gamma = 60^\circ$, and $\gamma = 30^\circ$ correspond to the prolate ($r_1 = r_2 < r_3$), oblate ($r_1 < r_2 = r_3$), and maximum triaxiality ($2r_2 = r_1 + r_3$) cases. Traditionally, the shapes of nuclei are inferred from low-energy spectroscopic measurements, which determine the shape parameters (β, γ) for even-even nuclei such as ^{208}Pb [35]. The shape of odd-mass nuclei such as ^{129}Xe can only be calculated using nuclear structure models that have been tuned to describe the even-even nuclei data. In this sense, flow measurements in high-energy heavy-ion collisions serve as a new tool to probe the nuclear shape, in particular for odd-mass nuclei. Recent model studies show that the v_2 and ρ_2 follow a simple parametric form [29,32,36],

$$v_2^2 \approx a + b\beta^2, \quad \rho_2 \approx a' + b'\cos(3\gamma)\beta^3. \qquad (3)$$

The parameters a and a' represent values for collisions of spherical nuclei. They are the smallest in central collisions, whereas the parameters b and b' are nearly independent of centrality. Therefore, the impact of nuclear deformation is expected to be largest in central collisions. A large quadruple deformation for ^{129}Xe of $\beta_{\rm Xe} \approx 0.16$–$0.2$ was extracted from the enhanced ratio $v_{2,\rm Xe}/v_{2,\rm Pb}$ in central collisions [37–39]. The measurement of ρ_2 here can then be used to further constrain the triaxiality of ^{129}Xe.

This paper studies the centrality and system-size dependences of ρ_n in ^{129}Xe + ^{129}Xe and ^{208}Pb + ^{208}Pb collisions to shed light on the effects of initial-state geometry and nuclear deformation. The measurements are performed in several ranges of p_T and η to quantify the influence of final-state effects [21]. The ρ_n values are also influenced by nonflow effects from resonance decays and jets, which can be suppressed using the "subevent method" [40,41], where the correlations are constructed by using particles from different subevents separated in η. The previous ALICE measurement of ρ_2 in Xe + Xe collisions [25] was performed in wide centrality ranges with limited statistical precision. The larger acceptance of the ATLAS detector and a factor of 10 more Xe + Xe events enable more precise measurements of ρ_2 in finer centrality ranges. A comparison of results in Xe + Xe and Pb + Pb collisions and model predictions then provides insight into the nuclear deformation and the nature of the initial sources responsible for harmonic flow and radial flow.

This paper also explores the issue of "centrality fluctuations," which refers to the fact that an experimental centrality definition based on the final-state particle multiplicity in an η range is subject to smearing due to fluctuations in the particle production process. Such centrality fluctuations, also known as volume fluctuations [42,43], have been shown to affect flow fluctuations [44,45] and ρ_n values [21,30,46]. This analysis explores the influence of centrality fluctuations on ρ_n using two reference event-activity estimators: the total transverse energy ΣE_T in the forward pseudorapidity range $3.2 < |\eta| < 4.9$ and the number of reconstructed charged particles, $N_{\rm ch}^{\rm rec}$, in the mid-rapidity range $|\eta| < 2.5$. Previous measurements of flow fluctuations show that ΣE_T has better centrality resolution than $N_{\rm ch}^{\rm rec}$ [45]. This conclusion was also reached by model investigations of the forward-backward multiplicity correlation in Pb + Pb collisions [47,48]. Therefore, the default results are obtained using ΣE_T, while those based on $N_{\rm ch}^{\rm rec}$ give a sense of the extent of centrality fluctuations.

The paper is organized as follows. Sections II and III describe details of the detector, event, and track selections. Section IV introduces the observables and subevent methods used in this analysis. The correlation analysis and systematic uncertainties are described in Secs. V and VI, respectively. Section VII presents the results of ρ_n in the two collision systems, and discusses the role of nonflow and centrality fluctuations. Section VIII compares the results with model predictions. A summary is given in Sec. IX.

II. ATLAS DETECTOR AND TRIGGER

The ATLAS detector [49] provides nearly full solid-angle coverage with tracking detectors, calorimeters, and muon chambers, and is well suited for measurements of multiparticle correlations over a large pseudorapidity range. The measurements are performed using the trigger system, the inner detector (ID), the forward calorimeters (FCal), and the zero-degree calorimeters (ZDC). The ID detects charged particles within $|\eta| < 2.5$ using a combination of silicon pixel detectors, silicon microstrip detectors (SCT), and a straw-tube transition-radiation tracker, all immersed in a 2 T axial magnetic field. The FCal consists of three sampling layers, longitudinal in shower depth, and covers $3.2 < |\eta| < 4.9$. The ZDC are positioned at ± 140 m from the IP, detecting neutrons and photons with $|\eta| > 8.3$. An extensive software suite [50] is used in the reconstruction and analysis of real and simulated data, in detector operations, and in the trigger and data acquisition systems of the experiment.

The ATLAS trigger system [51] consists of a level-1 (L1) trigger implemented in dedicated electronics and programmable logic, and a high-level trigger (HLT) which uses software algorithms similar to those applied in the offline event reconstruction. During Xe + Xe data-taking, the minimum-bias trigger selected events with either more than 4 GeV of transverse energy recorded in the whole calorimeter system at L1 (E_T^{L1}) or a reconstructed track with

$p_{\mathrm{T}} > 0.2$ GeV at the HLT. In the Pb + Pb data-taking, the minimum-bias trigger required either $E_{\mathrm{T}}^{\mathrm{L1}} > 50$ GeV or the presence of at least one neutron on both sides of the ZDC and a track identified by the HLT. To enhance the number of recorded events for ultracentral Pb + Pb collisions, a dedicated trigger selected on the $E_{\mathrm{T}}^{\mathrm{L1}}$ and the total transverse energy in the FCal, ΣE_{T}, at the HLT. The combined trigger selects events with ΣE_{T} larger than one of the three threshold values: 4.21, 4.37, and 4.54 TeV. The ultracentral trigger has a sharp turn-on as a function of ΣE_{T}, and for these thresholds the trigger is fully efficient for the 1.3%, 0.5%, and 0.1% of events in centrality percentile to be defined below, respectively. The fraction of events containing more than one inelastic interaction (pileup) is around 0.003 in Pb + Pb data and around 0.0002 in Xe + Xe data.

III. EVENT AND TRACK SELECTION

The analysis is based on ATLAS datasets corresponding to integrated luminosities of 3 $\mu\mathrm{b}^{-1}$ of minimum-bias Xe + Xe data recorded at $\sqrt{s_{NN}} = 5.44$ TeV in 2017 and 22 $\mu\mathrm{b}^{-1}$ of minimum-bias and 470 $\mu\mathrm{b}^{-1}$ of ultracentral Pb + Pb data recorded at $\sqrt{s_{NN}} = 5.02$ TeV in 2015. The offline event selection requires a reconstructed primary vertex with its z position satisfying $|z_{\mathrm{vtx}}| < 100$ mm. For the Pb + Pb dataset, pileup events are suppressed by exploiting the expected correlation between the estimated number of neutrons in the ZDC and $N_{\mathrm{ch}}^{\mathrm{rec}}$. For both the Pb + Pb and Xe + Xe datasets, a requirement is also imposed on the correlation between ΣE_{T} and $N_{\mathrm{ch}}^{\mathrm{rec}}$ to further reduce the number of background events. The events are classified into centrality intervals based on the ΣE_{T} in the FCal. A Glauber model [52,53] is used to parametrize the ΣE_{T} distribution and provide a correspondence between the ΣE_{T} distribution and the sampling fraction of the total inelastic Pb + Pb or Xe + Xe cross section, allowing centrality percentiles to be set. This analysis is restricted to the 0–84% most central collisions, where the triggers are fully efficient and the contamination from photonuclear processes is small [54]. This centrality range corresponds to $\Sigma E_{\mathrm{T}} > 0.042$ TeV in Pb + Pb collisions and $\Sigma E_{\mathrm{T}} > 0.03$ TeV in Xe + Xe collisions.

Charged-particle tracks [55] are reconstructed from hits in the ID, and are subsequently used to construct the primary vertices. Tracks are required to have $p_{\mathrm{T}} > 0.5$ GeV and $|\eta| < 2.5$ in Pb + Pb collisions and $p_{\mathrm{T}} > 0.3$ GeV and $|\eta| < 2.5$ in Xe + Xe collisions. They are required to satisfy the "loose" selection criteria, which require at least one pixel hit, with the additional requirement of a hit in the first pixel layer when one is expected, and at least six SCT hits. In addition, the distances of closest approach of the track to the primary vertex in both the transverse and longitudinal directions, $|d_0|$ and $|z_0 \sin\theta|$, are required to be less than 1.5 mm [56]. For evaluation of systematic uncertainties, the "tight" selection criteria are used, which further require at least two pixel hits, eight SCT hits, no missing hits in the pixel or SCT layers, and $|d_0|$ and $|z_0 \sin\theta|$ values both smaller than 1 mm. The primary particles in this analysis are defined as those with a lifetime larger than 30 picoseconds. The influence of secondary particles originating from weak decays and detector material interactions are accounted for by varying track selection criteria and efficiency correction [57].

The efficiency, $\epsilon(p_{\mathrm{T}}, \eta)$, of the track reconstruction and track selection criteria is evaluated using Pb + Pb and Xe + Xe Monte Carlo events produced with the HIJING event generator [58]. The generated particles in each event are rotated in azimuthal angle according to the procedure described in Ref. [59] to produce a harmonic flow consistent with the previous ATLAS measurements [10,56]. The response of the detector is simulated using GEANT4 [60,61] and the resulting events are reconstructed with the same algorithms as applied to the data. At mid-rapidity ($|\eta| < 1$), the efficiency for central Pb + Pb collisions is about 67% at 0.5 GeV and increases to 71% at higher p_{T}, while the efficiency for central Xe + Xe collisions is about 61% at 0.3 GeV and increases to 73% at higher p_{T} [39]. For $|\eta| > 1$, the efficiency decreases to about 40–60% depending on the p_{T} and centrality. The rate of falsely reconstructed ("fake") tracks is also estimated and found to be significant only at $p_{\mathrm{T}} < 1$ GeV in central collisions, where it ranges from 2% for $|\eta| < 1$ to 8% at larger $|\eta|$. The fake rate drops rapidly for higher p_{T} and for more peripheral collisions. The fake rate is accounted for in the tracking efficiency correction following the procedure in Ref. [62].

IV. OBSERVABLES

In the experimental analysis, the measurement of ρ_n in Eq. (1) requires a calculation of the individual components in the numerator and denominator. For this purpose, Eq. (1) is reexpressed as

$$\rho_n = \frac{\mathrm{cov}_n}{\sqrt{\mathrm{var}\left(v_n^2\right)\sqrt{c_k}}}, \quad \mathrm{cov}_n = \left\langle\left\langle v_n^2 \delta p_{\mathrm{T}}\right\rangle\right\rangle,$$
$$\mathrm{var}\left(v_n^2\right) = \left\langle v_n^4\right\rangle - \left\langle v_n^2\right\rangle^2, \quad c_k = \langle\langle \delta p_{\mathrm{T}} \delta p_{\mathrm{T}}\rangle\rangle. \tag{4}$$

The covariance cov_n is a three-particle correlator, which is obtained by averaging over unique triplets in each event and then over all events in an event-activity class based on $N_{\mathrm{ch}}^{\mathrm{rec}}$ or ΣE_{T}:

$$\mathrm{cov}_n = \left\langle \frac{\sum_{i,j,k,i\neq j\neq k} w_i w_j w_k e^{in(\phi_i - \phi_j)} (p_{\mathrm{T,k}} - \langle [p_{\mathrm{T}}]\rangle)}{\sum_{i,j,k,i\neq j\neq k} w_i w_j w_k} \right\rangle.$$

In the above formula, the indices i, j, and k loop over distinct charged particles to account for all unique triplets. The particle weight w is constructed to correct for both detector nonuniformities and tracking inefficiency as explained in Sec. V. The above expression for cov_n can be expanded algebraically within the cumulant framework [40,41,63,64] into a polynomial function of flow vectors and momentum-scalar quantities,

$$\mathbf{q}_{n;k} = \frac{\sum_i w_i^k e^{in\phi_i}}{\sum_i w_i^k},$$
$$p_{m;k} = \frac{\sum_i w_i^k (p_{\mathrm{T},i} - \langle [p_{\mathrm{T}}]\rangle)^m}{\sum_i w_i^k}, \tag{5}$$
$$[p_{\mathrm{T}}] = \frac{\sum_i w_i p_{\mathrm{T},i}}{\sum_i w_i},$$

with k and m being integer powers. Details of this expansion can be found in Ref. [65].

In order to reduce short-range nonflow correlations from resonance decays and jets, pseudorapidity gaps are often explicitly required between the particles in each triplet. This analysis uses the standard, two-subevent, and three-subevent methods to explore the influence of nonflow correlations [40,65]. In the standard method, all charged particles within $|\eta| < 2.5$ are used. In the two-subevent method, triplets are constructed by combining particles from two subevents labeled a and c, separated by a $\Delta\eta$ gap in between to reduce nonflow effects: $-2.5 < \eta_a < -0.75,\ 0.75 < \eta_c < 2.5$. The two particles contributing to the flow vector are chosen as one particle each from a and c, while the third particle providing the p_{T} is taken from either a or c. In the three-subevent method, three nonoverlapping subevents a, b, and c are chosen as $-2.5 < \eta_a < -0.75,\ |\eta_b| < 0.5,\ 0.75 < \eta_c < 2.5$. The particles contributing to flow are chosen from subevents a and c while the third particle is taken from subevent b.

In the large collision systems considered in this analysis, the nonflow effects are important only in peripheral collisions, where the statistical uncertainties of cov_n are also large. The cov_n values obtained from the two- and three-subevent methods agree within a few percent in mid-central and central collisions but show some differences in the peripheral region. In that region, however, only cov_2 has enough statistical precision to detect differences between the two- and three-subevent methods. Therefore, the final results for cov_2 are obtained from the three-subevent method, while the final results for cov_3 and cov_4 are obtained using triplets from both the two- and three-subevent methods, referred to as the "combined-subevent" method.

The statistical uncertainty of the measurement is obtained using a standard Poisson bootstrap method commonly employed in cumulant analyses [66,67]. Thirty pseudodatasets were generated by assigning to each event a random Poisson weight with a mean of 1, and the quantities in Eq. (4) are calculated for each pseudodataset. This method is mathematically justified when the number of events in a given event-activity class is sufficiently large. The standard deviations of the thirty values for each quantity were taken as the statistical uncertainties in the final result.

To obtain the Pearson coefficient in Eq. (4), one also needs to calculate the variances c_k and $\mathrm{var}(v_n^2)$. The former,

$$c_k = \left\langle \sum_{i,j,i\neq j} w_i w_j (p_{\mathrm{T,i}} - \langle [p_{\mathrm{T}}] \rangle)(p_{\mathrm{T,j}} - \langle [p_{\mathrm{T}}] \rangle) \right\rangle \Big/ \left\langle \sum_{i,j,i\neq j} w_i w_j \right\rangle,$$

is obtained using all the pairs in the full event, i.e. within $|\eta| < 2.5$. The latter is calculated in terms of the two-particle cumulant $c_n\{2\} \equiv \langle v_n^2 \rangle$ and four-particle cumulant $c_n\{4\} \equiv \langle v_n^4 \rangle - 2\langle v_n^2 \rangle^2$ [68],

$$\mathrm{var}\left(v_n^2\right) = c_n\{4\}_{\mathrm{standard}} + c_n\{2\}^2_{\mathrm{two\text{-}sub}}.$$

The $c_n\{4\}$, being four-particle correlators, are known to be relatively insensitive to nonflow correlations but usually have poor statistical precision [63]. Therefore, they are obtained from the standard method in the full event. On the other hand, the two-particle cumulants $c_n\{2\}$ are more susceptible to nonflow correlations but at the same time provide better statistical precision. Therefore, the $c_n\{2\}$ are calculated from the two-subevent method with the η choices discussed above. The calculation of $c_n\{2\}$ and $c_n\{4\}$ follow the procedure used in previous analyses [40,63], i.e., they are expressed in terms of flow vectors $\mathbf{q}_{n;k}$ defined in Eq. (5).

The default η ranges for the standard and subevent methods discussed above are listed in Table I. In addition to these default values, the analysis is also repeated for η ranges that are closer to mid-rapidity in order to study the impact of nonflow and longitudinal dynamics. This choice, listed in Table I as "Alternative η selection," could also be useful when comparing the results of this analysis with other experiments.

The charged particles used in this analysis are selected from some predefined p_{T} ranges similar to those in a previous measurement [24]. For the analysis of Pb + Pb data, two ranges, $0.5 < p_{\mathrm{T}} < 5$ GeV and $0.5 < p_{\mathrm{T}} < 2$ GeV, are used. For the analysis of Xe + Xe data, one additional range with a lower threshold, $0.3 < p_{\mathrm{T}} < 2$ GeV is used. However, the primary results are based on the range $0.5 < p_{\mathrm{T}} < 5$ GeV, which has the best statistical precision.

V. ANALYSIS PROCEDURE

The measurement of cov_n, $\mathrm{var}(v_n^2)$, and c_k follows a procedure similar to that detailed in Refs. [24,69] that consists of three steps. In the first step, these correlators are calculated in each event as the average over all combinations among particles from an η range and a p_{T} range listed in Table I. In the second step, the values obtained in each event are averaged over events with comparable multiplicity, defined as events with either similar ΣE_{T} values ($|\Delta\Sigma E_{\mathrm{T}}| < 0.002$ TeV) or the same $N_{\mathrm{ch}}^{\mathrm{rec}}$. They are then combined in broader multiplicity ranges of the event ensemble to obtain statistically more precise results. The Pearson coefficients ρ_n are then obtained via Eq. (4). This event-averaging procedure is necessary to reduce the effects of centrality fluctuations for each event-activity estimator [21,44,46].

In the third step, the $N_{\mathrm{ch}}^{\mathrm{rec}}$ dependence is converted to a centrality percentile dependence for each observable [24]. This is accomplished by calculating the average ΣE_{T} for each given $N_{\mathrm{ch}}^{\mathrm{rec}}$, which is then mapped to the centrality percentile. The mapping procedure is necessary such that results obtained for ΣE_{T} and $N_{\mathrm{ch}}^{\mathrm{rec}}$ can be directly compared using a common x axis.

In order to account for detector inefficiencies and nonuniformities, particle weights defined in Sec. IV are calculated as

$$w(\phi, \eta, p_{\mathrm{T}}) = d(\phi, \eta)/\epsilon(\eta, p_{\mathrm{T}}). \tag{6}$$

The additional weight factor $d(\phi, \eta)$ accounts for nonuniformities in the azimuthal acceptance of the detector as a function of η and amounts to a 5–20% variation. To determine it, all reconstructed charged particles for a given p_{T} selection are entered in a two-dimensional histogram $N(\phi, \eta)$, and the weight factor is then obtained as $d(\phi, \eta) \equiv \langle N(\eta) \rangle / N(\phi, \eta)$, where $\langle N(\eta) \rangle$ is the track density averaged over ϕ in the given η bin. This procedure removes most ϕ-dependent

TABLE I. The η and p_{T} ranges chosen for the standard and subevent methods.

Method	Default η selection	Alternative η selection
Standard	$\lvert\eta\rvert < 2.5$	$\lvert\eta\rvert < 1$
Two-subevent	$0.75 < -\eta_a, \eta_c < 2.5$	$0.35 < -\eta_a, \eta_c < 1$
Three-subevent	$0.75 < -\eta_a, \eta_c < 2.5, \lvert\eta_b\rvert < 0.5$	$0.35 < -\eta_a, \eta_c < 1, \lvert\eta_b\rvert < 0.3$
Combined-subevent	average of two-subevent and three-subevent results	
	p_{T} selection for Xe + Xe	p_{T} selection for Pb + Pb
	$0.3 < p_{\mathrm{T}} < 2$ GeV, $0.5 < p_{\mathrm{T}} < 5$ GeV, $0.5 < p_{\mathrm{T}} < 2$ GeV	$0.5 < p_{\mathrm{T}} < 5$ GeV, $0.5 < p_{\mathrm{T}} < 2$ GeV

nonuniformity from the track reconstruction [70], and the resulting flow vectors $\mathbf{q}_{n;k}$ in Eq. (5) should ideally be uniformly distributed in azimuthal angle. Any residual offsets are then subtracted by an event-averaged offset $\mathbf{q}_{n;k} - \langle \mathbf{q}_{n;k} \rangle_{\mathrm{evts}}$ [13], which was implemented as an improvement over the previous measurement [24].

VI. SYSTEMATIC UNCERTAINTIES

The systematic uncertainties in this analysis arise from track selection, reconstruction efficiency, acceptance reweighting and centrality selection, and are evaluated for each observable: cov_n, $\mathrm{var}(v_n^2)$, c_k, and ρ_n. Systematic uncertainties from many sources enter the analysis through the particle weights in Eq. (5). The uncertainties partially cancel out between the numerator and denominator in constructing ρ_n. The uncertainties quoted below are for the 0–50% centrality range, and they are generally comparable between Xe + Xe and Pb + Pb. In the peripheral collisions, systematic uncertainties are smaller than the statistical uncertainties; they are evaluated but not quoted below because ρ_n values are often very close to zero, and quoting the uncertainties as percentages is not very meaningful. The uncertainty contributions from different sources are described below with a focus of their impact on ρ_n.

From previous measurements [10], the v_n signal has been shown to have a strong dependence on p_{T} but relatively weak dependence on η. Therefore, a p_{T}-dependent uncertainty in the track reconstruction efficiency $\epsilon(\eta, p_{\mathrm{T}})$ could affect the measured signal through the particle weights. The uncertainties in the track reconstruction efficiency are due to differences in the detector conditions and known differences in the material between data and simulations. The uncertainties in detector efficiency vary in the range 1–4%, depending on η and p_{T} [39,71]. The systematic uncertainties for each observable are evaluated by repeating the analysis with the tracking efficiency increased and decreased by its corresponding uncertainty. The resulting uncertainties in ρ_n are less than 2% for $n = 2$ and 4, but increase to 6% for $n = 3$ because the cov_3 values decrease towards zero in the peripheral region.

The contamination from fake tracks varies with the tracking selection. To assess how the fake tracks change the results, the requirements imposed on the reconstructed tracks are varied from those in the default track selection. The loose and tight track selections discussed in Sec. III are used for this purpose. The differences are largest in the most central and peripheral collisions, where the correlation signals are smaller and the influence of fake tracks is thus higher. In Pb + Pb collisions, the differences are up to 3%, 6%, and 9% for $n = 2$, 3, and 4, respectively. The uncertainties are smaller in Xe + Xe collisions due to lower rates of fake tracks, except in peripheral collisions for $n = 3$ and 4.

The effect of detector azimuthal nonuniformity is accounted for by the weight factor $d(\eta, \phi)$ in Eq. (6). The effect of reweighting is studied by setting the weight to 1 and repeating the analyses with the residual offset correction still applied to the flow vectors. The unweighted results generally agree with the weighted results within 1–3%, except for peripheral Xe + Xe collisions, where the uncertainties are larger.

The centrality definitions used to classify the events into centrality percentiles in the 0–84% range have a 1% uncertainty, due to an inefficiency in selecting minimum-bias collisions. The impact of this uncertainty is evaluated by varying the centrality interval definitions by ±1%, and recalculating all the observables. The impact for all observables is small in central and mid-central collisions, but becomes the dominant uncertainty in the more peripheral region. This type of uncertainty is only used when results are presented as a function of centrality percentiles. The uncertainties are 0–3% in central and mid-central collisions and increase to 2–8% in the more peripheral collisions depending on the harmonic number n and collision system.

The systematic uncertainties from the different sources described above are added in quadrature to give the total systematic uncertainty for each observable. These uncertainties for ρ_n are summarized in Table II. The relative uncertainties are larger in central and peripheral collisions, where the values of ρ_n are small relative to their statistical uncertainties.

VII. RESULTS

The values of c_k, $\mathrm{var}(v_n^2)$, and cov_n are calculated and combined to obtain ρ_n for each choice of p_{T} and η ranges in Pb + Pb and Xe + Xe collisions as defined in Table I. In each case, they can be obtained with the event-averaging procedure in intervals of either ΣE_{T} or $N_{\mathrm{ch}}^{\mathrm{rec}}$ and those intervals are translated to average centrality values. The default event-averaging procedure is based on ΣE_{T}. As described in Sec. IV, the primary results shown are calculated for charged particles in the range $0.5 < p_{\mathrm{T}} < 5$ GeV, using the three-subevent method for ρ_2 and the combined-subevent method for ρ_3 and ρ_4.

TABLE II. Sources of systematic uncertainty in percentage on the measured ρ_n values.

Centrality	Sources	Pb + Pb			Xe + Xe		
		ρ_2 (%)	ρ_3 (%)	ρ_4 (%)	ρ_2 (%)	ρ_3 (%)	ρ_4 (%)
0–10%	Efficiency	0.9	2.2	1.5	0.5	1.4	1.2
	Track quality	0.5	0.6	9	0.6	4.9	0.7
	ϕ nonuniformity	0.5	<0.5	0.9	1	<0.5	2.3
	Centrality	<0.5	<0.5	1.5	<0.5	<0.5	0.5
	Total	2	3	10	2	6	3
20–30%	Efficiency	1.2	3	0.9	1.0	3.2	0.8
	Track quality	1.6	3.6	1.5	<0.5	2.3	2.5
	ϕ nonuniformity	<0.5	<0.5	0.6	<0.5	1.5	<0.5
	Centrality	<0.5	3	1.5	<0.5	1.5	0.6
	Total	2	6	3	2	4	3
40–50%	Efficiency	1.3	6	0.8	<0.5	15	15
	Track quality	1.9	7.5	1.1	1.2	15	0.6
	ϕ nonuniformity	<0.5	<0.5	<0.5	<0.5	1.5	7
	Centrality	1.4	1.5	0.8	1.8	6	<0.5
	Total	3	10	2	3	22	18

A. Dependence on method and collision systems

Figure 1 shows the ρ_n values obtained from the standard, two-subevent, and three-subevent methods for charged particles with $0.5 < p_{\mathrm{T}} < 5$ GeV in Pb + Pb and Xe + Xe collisions. They are obtained using the event-averaging procedure based on ΣE_{T} and plotted as a function of centrality.

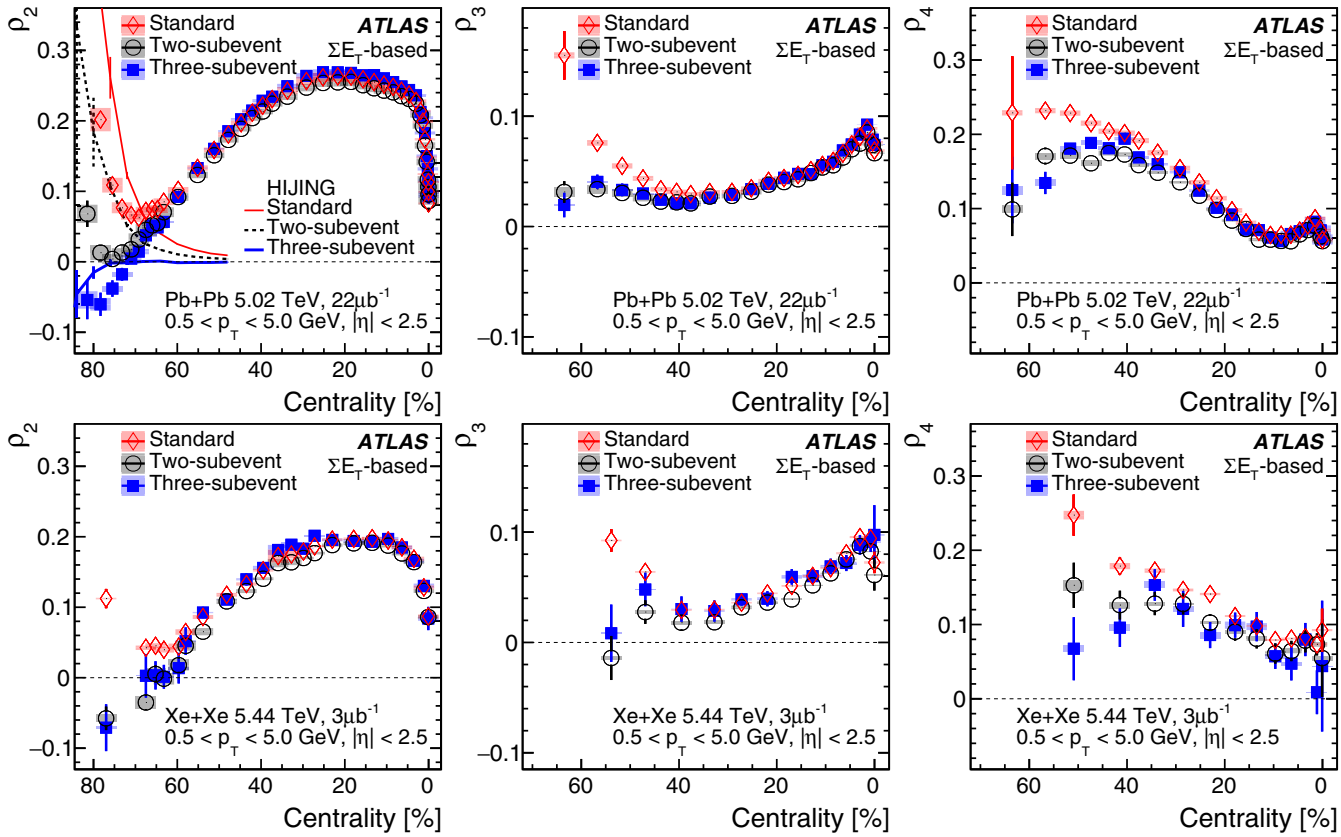

FIG. 1. The centrality dependence of ρ_n for $n = 2$ (left), 3 (middle), and 4 (right) in Pb + Pb (top) and Xe + Xe (bottom) collisions calculated for the standard, two-subevent, and three-subevent methods. They are calculated using the event-averaging procedure based on ΣE_{T}. The error bars and shaded boxes represent statistical and systematic uncertainties, respectively. To reduce the statistical fluctuations in the Xe + Xe data, wider centrality binning is used in the bottom row. The Pb + Pb ρ_2 data are also compared with HIJING calculations from Ref. [65], which includes only nonflow correlations.

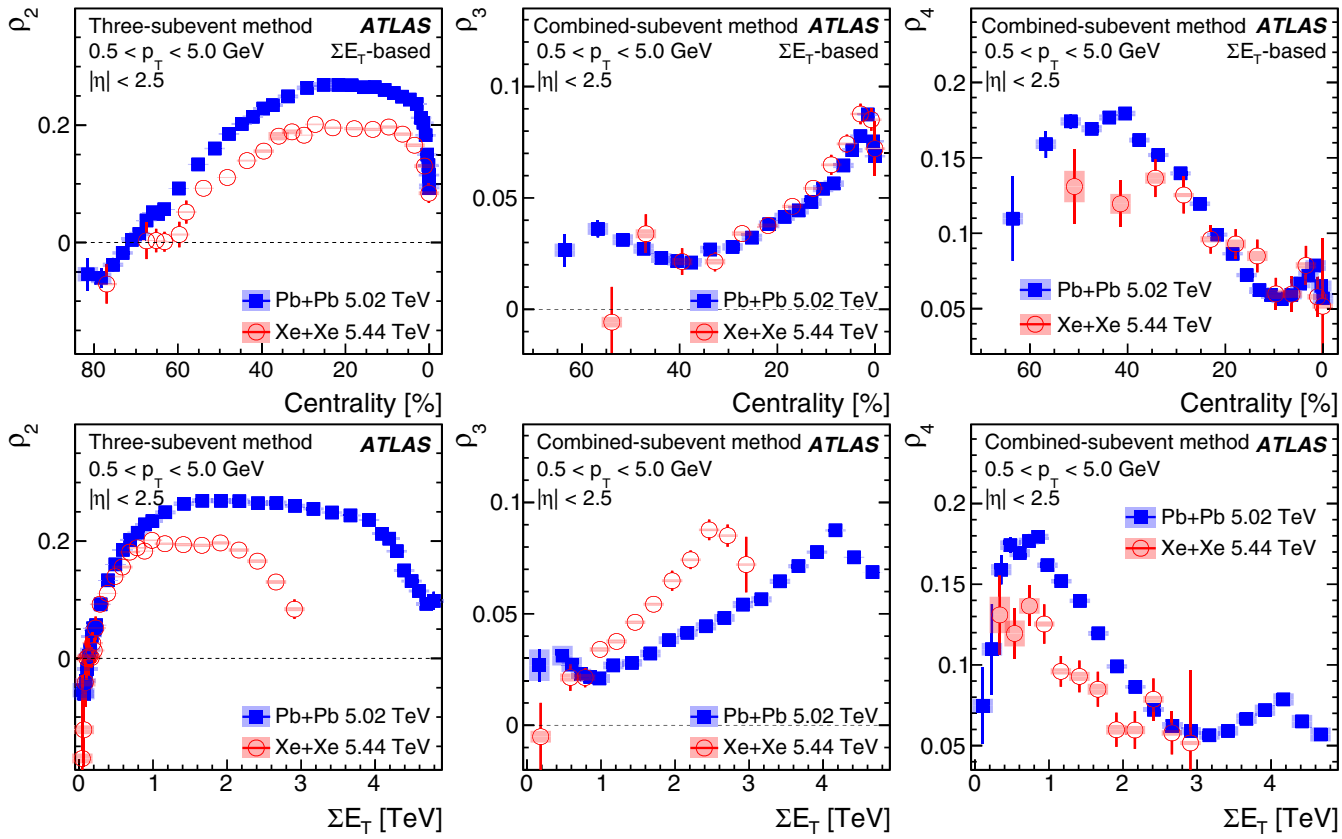

FIG. 2. The centrality (top) and ΣE_{T} (bottom) dependences of ρ_n for $n = 2$ (left), 3 (middle), and 4 (right) in Pb + Pb and Xe + Xe collisions. They are calculated using the event-averaging procedure based on ΣE_{T}. The error bars and shaded boxes represent statistical and systematic uncertainties, respectively.

The results are close to each other in central and mid-central collisions. In peripheral collisions beyond 60% centrality, the values from the standard method are significantly larger than those obtained from the subevent methods. This is consistent with the significant nonflow correlations arising from resonance decays and jets, which give positive contributions to both v_n and $[p_{\mathrm{T}}]$ in the standard method. The nonflow effects in the two-subevent method, reflected by the difference from the three-subevent method, are also visible beyond 70% centrality. Smaller differences, albeit weakly dependent on centrality, are also observed between the two-subevent method and the three-subevent method in mid-central and central collisions. These differences are expected because the v_n signal, as well as the decorrelations of v_n and $[p_{\mathrm{T}}]$, depend on the chosen η intervals and $\Delta\eta$, which differ between the two methods [20,72,73].

The influence of nonflow effects was investigated recently in models [65,74]. The ρ_2 obtained from the HIJING model, which generates only nonflow correlations, shows a similar ordering between the three methods, as seen in Fig. 1. In particular, the values of ρ_2 from the three-subevent method are closer to zero in the multiplicity range corresponding to the centrality range shown in Fig. 1. The ρ_2 signal in the peripheral region cannot be reproduced by the HIJING model, which only includes nonflow correlations.

The results from the subevent methods show similar centrality dependences between the Pb + Pb and Xe + Xe: the ρ_2 values reach a minimum in the peripheral collisions, increase to a positive maximum value, and then decrease in the most central collisions; the ρ_3 values show a mild increase towards central collisions; the ρ_4 values show an increase then a gradual decrease towards central collisions.

In the ultracentral collision region, all the ρ_n show a sharp decrease towards the most central collisions. This decrease is much clearer in the Pb + Pb system due to its superior statistical precision and better centrality resolution than in the Xe + Xe system. This sharp decrease starts at around 1.6% in centrality in Pb + Pb, which matches approximately to the location of the knee in the minimum-bias ΣE_{T} distribution [45]. For events having ΣE_{T} values beyond the knee, essentially all nucleons participate in the collision. As a result, geometric fluctuations that enhance the ρ_n values are suppressed. A similar suppression of fluctuations has also been observed for other flow observables [45].

Figure 2 provides a direct comparison of the Pb + Pb and Xe + Xe ρ_n values as a function of centrality (top) and ΣE_{T} (bottom). These two different choices for the x axis test whether the system-size dependence of ρ_n scales with centrality or event multiplicity. When compared at the same centralities, the Xe + Xe ρ_2 values are everywhere smaller than the Pb + Pb values. However, when compared using ΣE_{T}, the Pb + Pb and Xe + Xe ρ_2 values agree for small ΣE_{T} values ($\Sigma E_{\mathrm{T}} < 0.5$ TeV) but differ for larger ΣE_{T}. When plotted as a function of ΣE_{T}, the ρ_3 values in Pb + Pb and

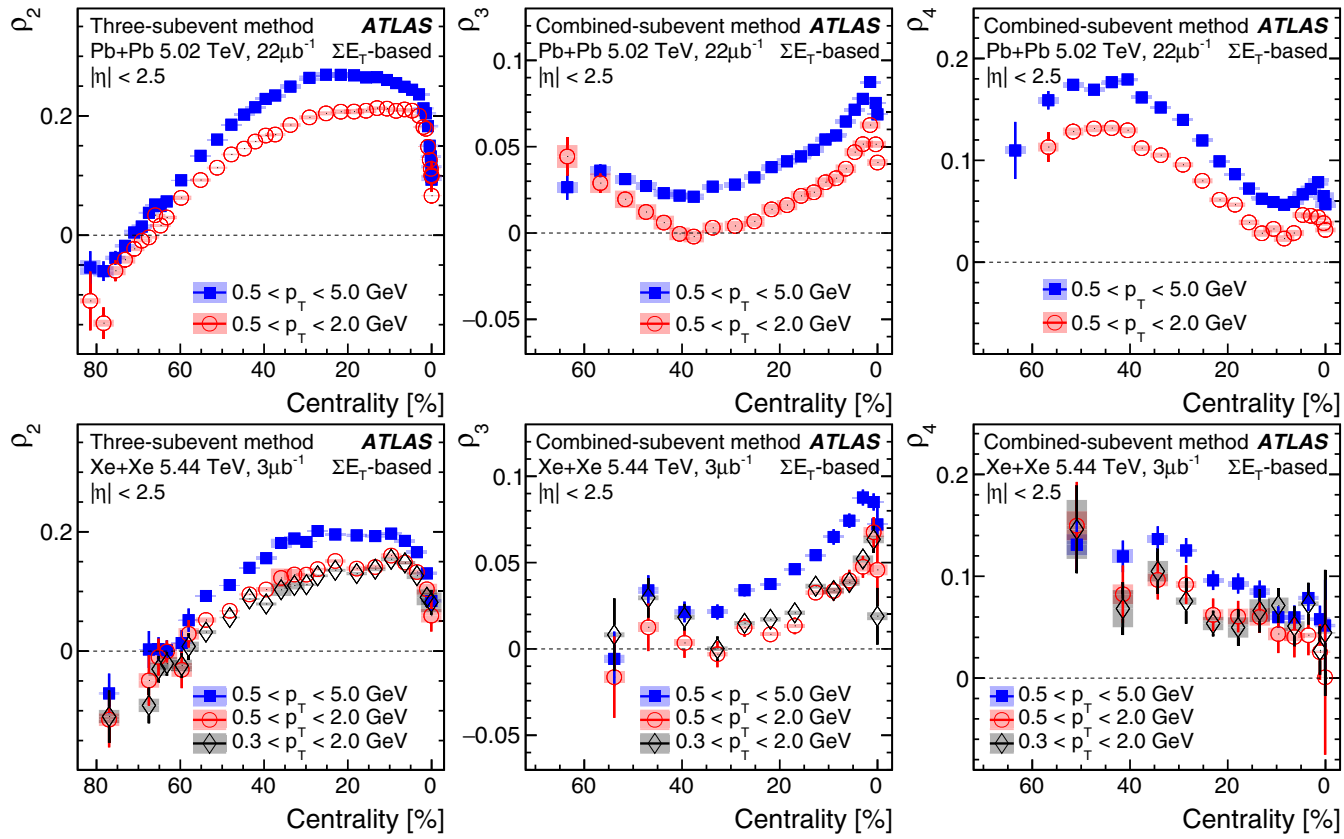

FIG. 3. The centrality dependence of ρ_n for two p_T ranges in Pb + Pb collisions (top) and three p_T ranges in Xe + Xe collisions (bottom) for $n = 2$ (left), 3 (middle), and 4 (right). They are obtained via the event-averaging procedure based on ΣE_T. The error bars and shaded boxes represent statistical and systematic uncertainties, respectively.

Xe + Xe collisions are similar only at low ΣE_T, while they are similar over the full range when plotted as a function of centrality. The ρ_4 values for the two systems are similar when plotted as a function of centrality in the 0–40% centrality range, but not when plotted as a function of ΣE_T.

B. Dependence on the p_T and η ranges

Figure 3 shows the centrality dependence of ρ_n in two p_T ranges for Pb + Pb collisions and three p_T ranges for Xe + Xe collisions. It is observed that the ρ_n values for $0.5 < p_T < 2$ GeV are smaller than those for $0.5 < p_T < 5$ GeV in both systems, but the overall centrality dependence remains similar. In Xe + Xe collisions, the ρ_n values obtained for a lower p_T range of $0.3 < p_T < 2$ GeV are found to be close to those obtained for $0.5 < p_T < 2$ GeV. This is expected since the collective behavior of the bulk particles in the $0.5 < p_T < 2$ GeV range reflects mainly hydrodynamic response, so including more particles by further lowering the p_T threshold does not significantly change the ρ_n. This is an important observation for comparison with other experiments or model calculations, where different p_T ranges are often used.

The analysis is also repeated for the η range closer to mid-rapidity, $|\eta| < 1$, as listed in Table I. Figure 4 compares the centrality dependence of ρ_n and cov_n for the two η ranges. The results for cov_n are almost in agreement with each other, except for $n = 2$ and 4 in peripheral collisions. In contrast, the results for ρ_n are systematically lower for $|\eta| < 1$ than for $|\eta| < 2.5$. This implies that the difference arises from the η dependence of the $\mathrm{var}(v_n^2)$ and c_k values used to calculate ρ_n via Eq. (5). The values of cov_2 and ρ_2 for centrality above 70% are larger for $|\eta| < 1$, likely due to larger residual nonflow effects associated with a smaller η range.

C. Effects of centrality fluctuations

As discussed in the introduction, due to the finite resolution of an event-activity estimator used to characterize the event centrality, the multiparticle cumulants for flow and $[p_T]$ fluctuations are sensitive to the multiplicity observable used in the event-averaging procedure. The results for ρ_n as a function of centrality in Pb + Pb and Xe + Xe collisions are shown in Fig. 5. Large differences between the ρ_2 values are observed in central collisions and in peripheral collisions: compared to results based on ΣE_T, the results based on $N_{\mathrm{ch}}^{\mathrm{rec}}$ are larger in central collisions (0–40% range) and smaller in peripheral collisions (beyond 50% centrality). Differences between the two event activities are also observed for ρ_3 and ρ_4.

The influence of centrality fluctuations on ρ_n was recently studied in a transport model framework [30], albeit at RHIC energies of $\sqrt{s_{NN}} = 0.2$ TeV. That study found that the ρ_2 values based on particle multiplicity at mid-rapidity are different from those based on particle multiplicity at forward rapidity. These differences are qualitatively similar to those observed in

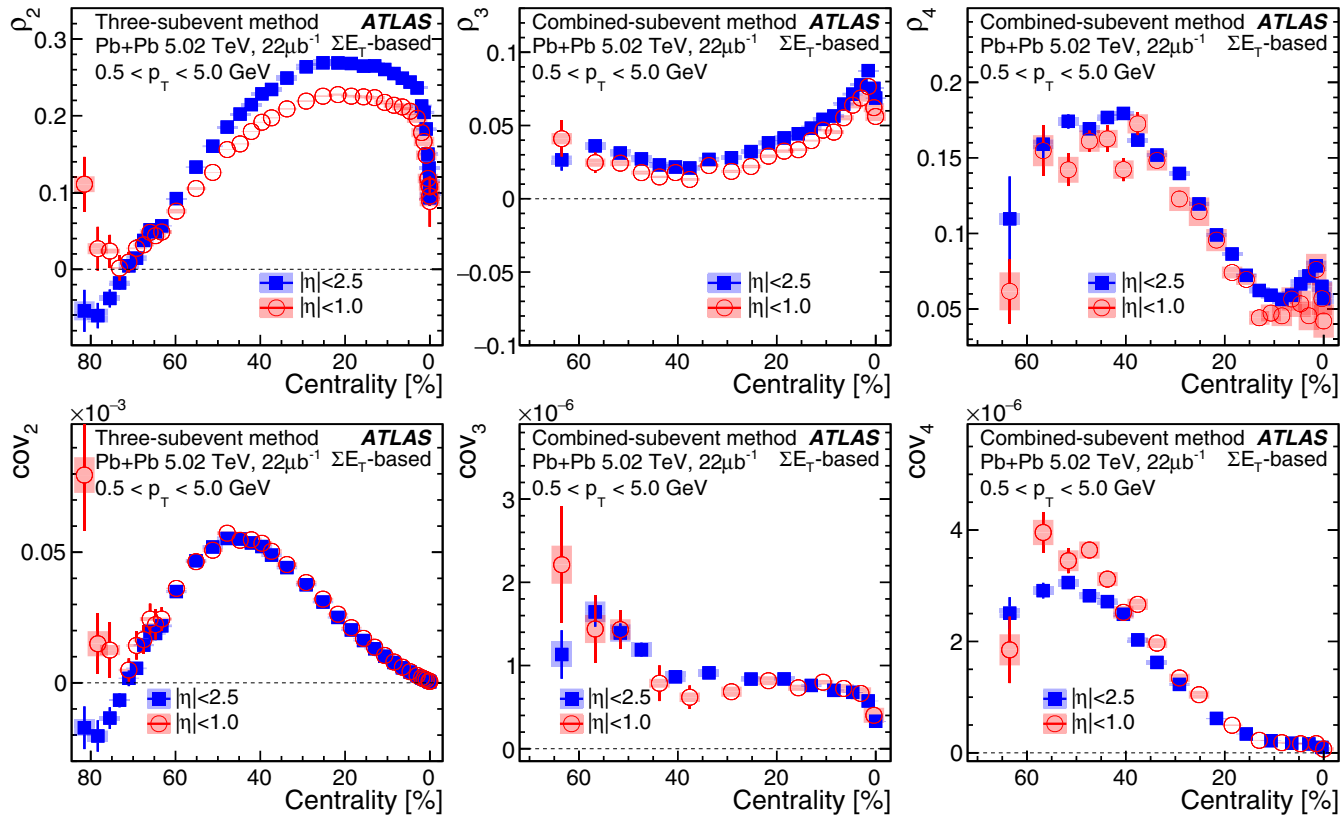

FIG. 4. The centrality dependence of ρ_n (top) and cov_n (bottom) for $n = 2$ (left), 3 (middle), and 4 (right) in Pb + Pb collisions compared between the two choices for the η ranges from Table I. They are calculated using the event-averaging procedure based on ΣE_{T}. The error bars and shaded boxes represent statistical and systematic uncertainties, respectively.

Fig. 5. The ρ_2 values obtained using event activity at forward rapidities were also found to be more consistent with results obtained using the number of participating nucleons [30]. That finding reinforces the notion that the event-activity estimator in ATLAS based on ΣE_{T} has better centrality resolution than the estimator based on $N_{\mathrm{ch}}^{\mathrm{rec}}$.

Recently, it was argued that ρ_2 is a sensitive probe of the nature of collectivity in small collision systems and peripheral heavy-ion collisions, in particular for isolating the contribution from initial momentum anisotropy in a gluon saturation picture [26]. The hydrodynamic expansion in the final state produces a negative (positive) ρ_2 in peripheral (nonperipheral) collisions [21,26,46], while the initial momentum anisotropy is expected to give a large positive contribution in the most peripheral collisions [22]. Therefore, the centrality dependence of ρ_2, after considering both the initial-state and final-state effects, is predicted to exhibit an increasing trend toward the most peripheral centrality [22]. However, Fig. 5 shows that the trends of ρ_2 in peripheral collisions could still be modified by the centrality fluctuations.

Figure 6 compares the centrality dependence of ρ_2 in $|\eta| < 2.5$ and $|\eta| < 1$ based on ΣE_{T} and $N_{\mathrm{ch}}^{\mathrm{rec}}$ in more detail over the 60–84% centrality range. It is shown separately for the standard method and subevent methods in order to better separate the influence of nonflow effects from other effects. The successive reduction of the ρ_2 from the standard method in the left panel, to the two-subevent method in the middle panel, and to the three-subevent method in the right panel is a robust feature of suppression of the nonflow correlations [65]. In the right panel, where the residual nonflow is the smallest, two interesting features can be observed: (1) the ρ_2 values obtained for the narrow $|\eta| < 1$ range are much larger than those for $|\eta| < 2.5$, suggesting that the results obtained in $|\eta| < 1$ still have significant nonflow contributions; (2) the differences between the ρ_2 values from the two event-activity estimators are large for both η ranges, reflecting the impact of centrality fluctuations. The results from this measurement do not show clear evidence for initial-state momentum anisotropy. Future more detailed studies of the behavior of ρ_2 in very peripheral collisions, including smaller pp and p + Pb collision systems, will be useful to disentangle the effects of nonflow, centrality fluctuations, and initial momentum anisotropy.

VIII. COMPARISON WITH THEORY

After the ρ_n observable was proposed [20], several model predictions became available with different assumptions about the initial condition and final-state dynamics. Models that consider only the initial condition, such as Glauber or Trento models [75], rely on a linear response relation between flow and eccentricity, $v_n \propto \varepsilon_n$, and between $[p_{\mathrm{T}}]$ and the ratio of initial energy to initial entropy, E/S [21,76]. From ε_n and E/S, which can be calculated for each event without running the full hydrodynamic model simulation, the authors construct

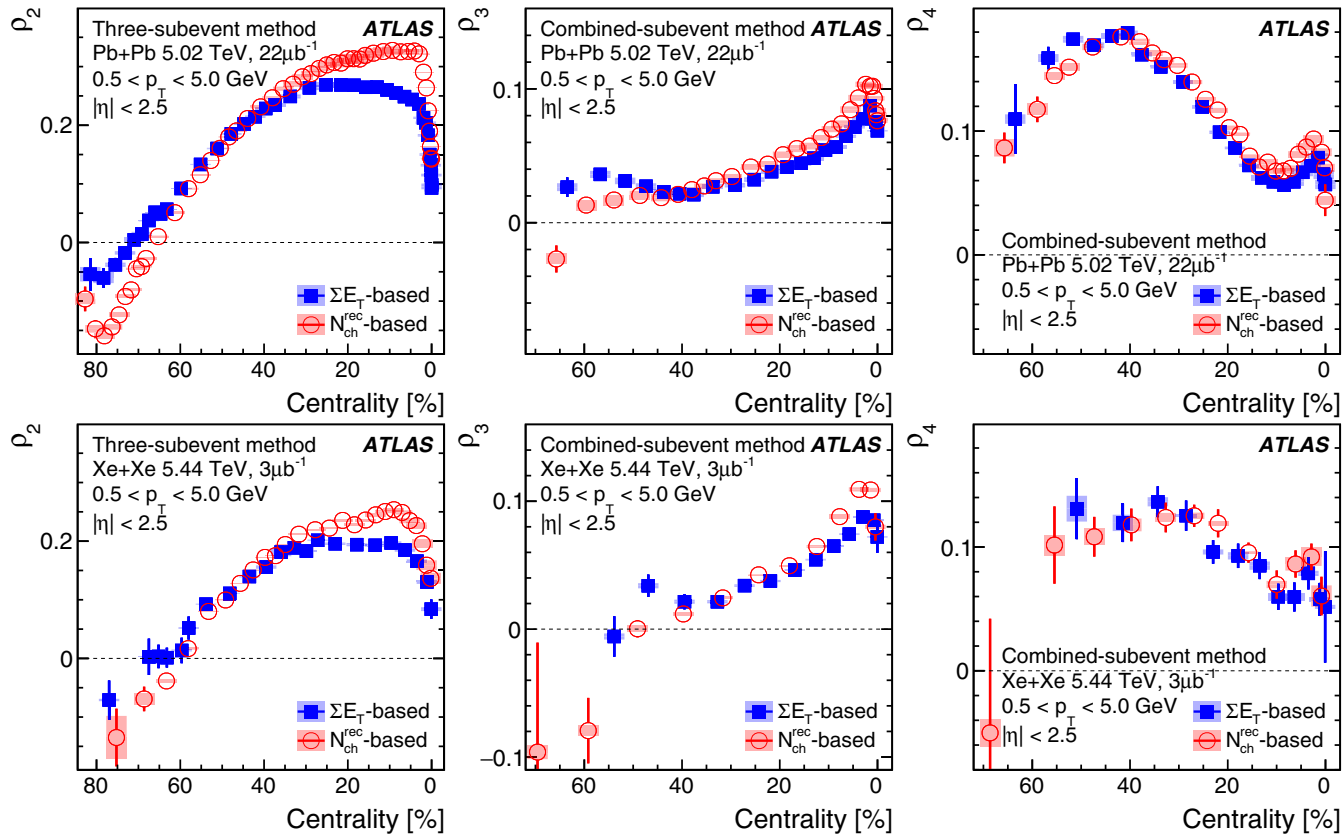

FIG. 5. The centrality dependence of ρ_n in Pb + Pb (top) and Xe + Xe (bottom) collisions for $n = 2$ (left), 3 (middle), and 4 (right), compared between the $N_{\mathrm{ch}}^{\mathrm{rec}}$-based event-averaging procedure (solid squares) and the ΣE_{T}-based event-averaging procedure (solid circles). The results are calculated using charged particles with $0.5 < p_{\mathrm{T}} < 5$ GeV. The error bars and shaded boxes represent statistical and systematic uncertainties, respectively.

an estimator for the ρ_n values. More realistic hydrodynamic models start from the Glauber or Trento model, and the system is evolved according to either two-dimensional (2D) boost-invariant or IP-Glasma full three-dimensional (3D) hydrodynamic equations. These models include the v-USPhydro model [26], the Trajectum model [77], and the IP-Glasma + MUSIC model [21,22]. The first two are 2D hydrodynamic models based on a Trento initial condition and the third is a 3D hydrodynamic model based on a 3D initial condition that is dynamically generated from gluon saturation models. The latter has an option to include the contribution from initial momentum anisotropy (ϵ_p). For comparison with the data, the predictions of IP-Glasma + MUSIC both with and without ϵ_p are included. Most models have been tuned to

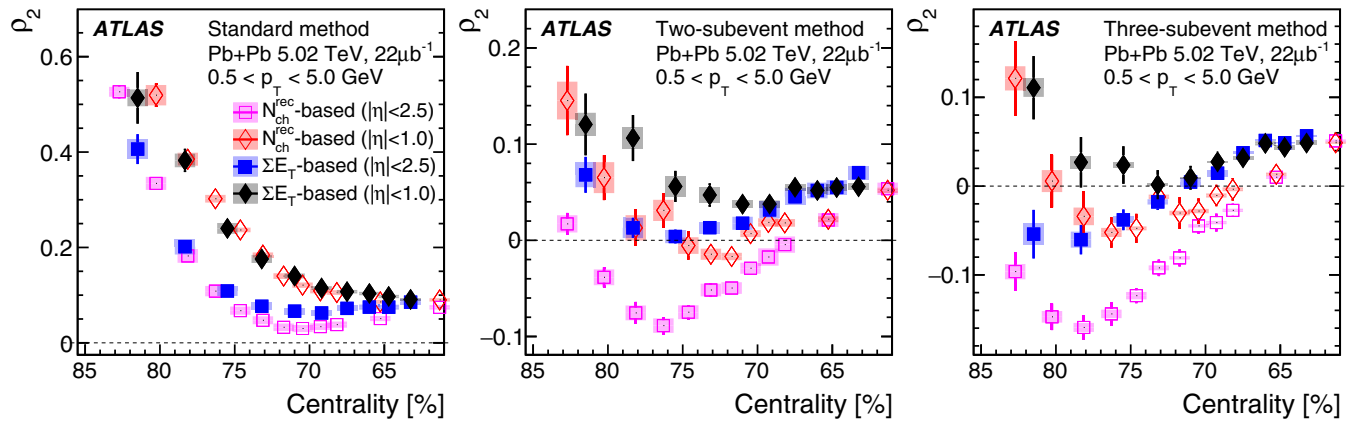

FIG. 6. The centrality dependence of ρ_2 in Pb + Pb collisions in the peripheral region of 60–84% for the standard method (left), two-subevent method (middle), and three-subevent method (right), compared between the $N_{\mathrm{ch}}^{\mathrm{rec}}$-based and ΣE_{T}-based event-averaging procedures and two η ranges. The error bars and shaded boxes represent statistical and systematic uncertainties, respectively.

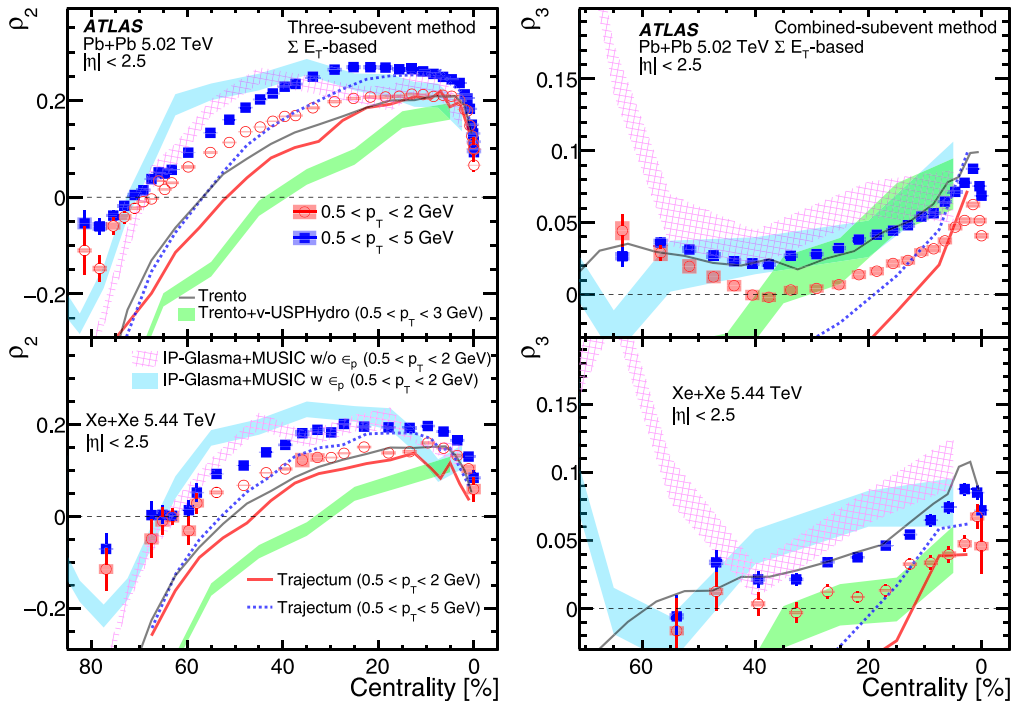

FIG. 7. The ρ_2 (left) and ρ_3 (right) values in Pb + Pb (top) and Xe + Xe (bottom) collisions in two p_T ranges and $|\eta| < 2.5$ compared with various models: Trento [76] and Trajectum [77] models in solid lines and v-USPhydro [26] and IP-Glasma + MUSIC [22] hydrodynamic models in shaded bands, which represent the statistical uncertainties of the model calculations.

describe reasonably well the bulk observables such as v_2, v_3, and p_T spectra. Many of these models also include the effects of nuclear quadrupole deformation with different values of the deformation parameters (β, γ) in Eq. (2). The chosen β_{Xe} value is 0.2 in Trento, 0.16 in Trajectum, and 0.18 in IP-Glasma + MUSIC. The chosen β_{Pb} value is 0.06 in Trento, but zero in other models. The default triaxiality value is chosen to be $\gamma_{Xe} = 30°$ and $\gamma_{Pb} = 27°$ in Trento and zero in other models. The choice of deformation parameter values in the Trento model is motivated by state-of-the-art nuclear energy-density functional calculations [31,78], which predict the most probable values of $(\beta_{Xe}, \gamma_{Xe}) \approx (0.2, 27°)$ and $(\beta_{Pb}, \gamma_{Pb}) \approx (0.06, 27°)$. However, these calculations also predict that the shapes of Pb and Xe nuclei are not fixed, and can fluctuate over a broad range of γ values. Figure 7 shows the ρ_2 and ρ_3 values for two p_T ranges in Pb + Pb (top) and Xe + Xe (bottom) collisions. They are compared with the various models described above.

In the 0–10% centrality interval, where the effects of nuclear deformation are important, all models generally show reasonable agreement with each other and with the data. In particular, the Trajectum model quantitatively reproduces the ordering between $0.5 < p_T < 2$ GeV and $0.5 < p_T < 5$ GeV. In central Xe + Xe collisions, however, the Trajectum model underestimates the ρ_2 values, probably due to the smaller value of β_{Xe} used. In noncentral collisions, these models show significant differences from each other, which were recently shown to mainly reflect the different parameter values for the initial condition, in particular the nucleon size [23]. In the peripheral collisions, all model predictions for ρ_2 show a sharp decrease and a sign change, qualitatively consistent with the ATLAS data. The Trento model, which includes only initial-state effects, by construction has no p_T or η dependencies for ρ_2. The results from this model underestimate the values of ρ_2 in all p_T ranges, describe the values of ρ_3 for $0.5 < p_T < 5$ GeV, and overestimate the values of ρ_3 in other p_T ranges. The v-USPhydro and Trajectum models significantly underestimate both the ρ_2 and ρ_3 values in noncentral collisions. IP-Glasma + MUSIC model predictions, both with and without ϵ_p included, are above the data in mid-central collisions (30–60% centrality), but are below the data in more peripheral collisions. The IP-Glasma + MUSIC model predicts the location for the sign change but overestimates the data in mid-central collisions. The IP-Glasma + MUSIC model with ϵ_p shows differences from the model without ϵ_p in peripheral collisions beyond 70% centrality, where the current data have limited precision. More detailed experimental measurements in that region, including smaller pp and p + Pb collision systems, are needed to clarify the role of initial momentum anisotropy.

Figure 8 compares ρ_2 data in the 0–20% centrality range with the Trento model calculations to investigate the influence of triaxiality [31]. Because of the large quadrupole deformation of the ^{129}Xe nucleus, $\beta_{Xe} \approx 0.2$, the ρ_2 should be sensitive to the triaxiality parameter γ_{Xe}. This expectation is confirmed in the Trento model which produces significantly different trends for ρ_2 as a function of centrality for different γ_{Xe} values. However, comparisons between the Trento model and data require care as the p_T dependence of ρ_n is absent in the Trento model.

In order to cancel out the p_T dependence in the data, ratios of ρ_2 values between Xe + Xe and Pb + Pb are calculated

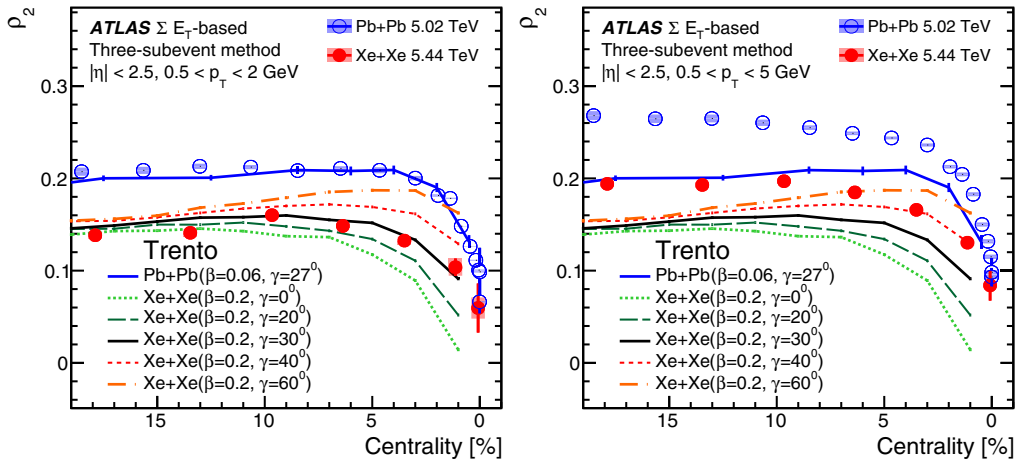

FIG. 8. Comparison of ρ_2 in Xe + Xe and Pb + Pb collisions with the Trento model for various quadrupole deformation parameter values [31] in $0.5 < p_T < 2$ GeV (left) and $0.5 < p_T < 5$ GeV (right) as a function of centrality. The same Trento results are used in both panels, and they are connected by lines for better visualization.

for the two p_T ranges and compared with the ratios obtained in the Trento model in Fig. 9. The ratio of the ρ_2 values is found to be approximately 0.7, and it is slightly lower in $0.5 < p_T < 2$ GeV than in $0.5 < p_T < 5$ GeV. In the 10–20% centrality range, where the triaxiality plays a minor role, the model calculation is very close to the data ratio. In the 0–10% centrality range, where the predicted ρ_2 values show significant dependence on the triaxiality, the comparison between the model and data favors a $\gamma_{Xe} \approx 30^\circ$. This comparison provides clear evidence that flow measurements in central heavy-ion collisions can be used to constrain the quadrupole deformation, including the triaxiality, of the colliding nuclei. A future detailed comparison of the ρ_2 ratio with precision state-of-the-art hydrodynamic model calculations for different values of the deformation parameters would be needed to extract the most probable β_{Xe} and γ_{Xe} values.

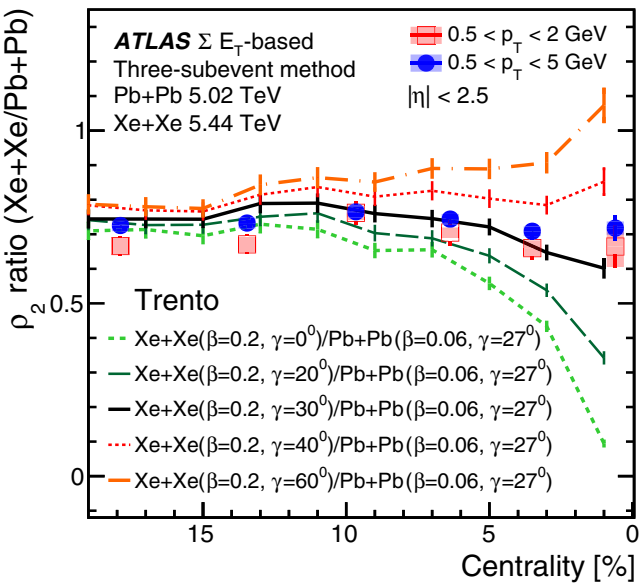

FIG. 9. Comparison of ρ_2 ratios, $\rho_{2,\mathrm{Xe+Xe}}/\rho_{2,\mathrm{Pb+Pb}}$, with the Trento model for various quadrupole deformation parameter values [31] in two p_T ranges. The Trento model results are connected by lines for better visualization.

IX. CONCLUSION

This paper presents a measurement of the correlation between harmonic flow and the mean transverse momentum using 22 (470) μb^{-1} of minimum-bias (ultracentral) Pb + Pb collisions at $\sqrt{s_{NN}} = 5.02$ TeV and 3 μb^{-1} of minimum-bias Xe + Xe collisions at $\sqrt{s_{NN}} = 5.44$ TeV recorded by the ATLAS detector at the LHC. The correlation between v_n^2 and the event-by-event $[p_T]$ is quantified using the Pearson correlation coefficient ρ_n, which is potentially sensitive to the shape and size of the initial geometry, nuclear deformation, and initial momentum anisotropy. Results are obtained for several p_T and η selections as a function of centrality, characterized by either N_{ch}^{rec}, the number of reconstructed charged particles in $|\eta| < 2.5$, or ΣE_T, the total transverse energy in the forward pseudorapidity range $3.2 < |\eta| < 4.9$. A comparison of results between these two event-activity estimators reveals the effects of centrality fluctuations.

The influence of nonflow contributions is studied using comparison between the standard, two-subevent, and three-subevent cumulant methods. The comparison between the three cumulant methods implies that the nonflow contribution has very little influence in the 0–70% centrality range in both systems when using the subevent method. However, the results obtained from a smaller η range, e.g., $|\eta| < 1$, using the subevent method may still have significant nonflow contributions in the peripheral collisions. The results show significant differences between the two event-activity estimators. In central collisions, the ρ_n values obtained with the N_{ch}^{rec}-based event-activity estimator are larger than those obtained with the ΣE_T-based estimator for all harmonics, while the opposite trend is observed in peripheral collisions. These differences

can be attributed to the relatively poorer centrality resolution associated with the $N_{\mathrm{ch}}^{\mathrm{rec}}$-based event-activity selection, which was also observed in previous flow measurements [45]. Therefore, results based on ΣE_{T} are chosen as default results to be compared with models.

The results are compared with the Trento model calculation, which considers effects associated with the initial-state geometry and nuclear deformation, and three hydrodynamic models, v-USPhydro, Trajectum, and IP-Glasma + MUSIC, which consider the full space-time dynamics. The IP-Glasma + MUSIC model also has the option to include the contribution from the initial momentum anisotropy. All these models qualitatively describe the overall centrality- and system-dependent trends but fail to quantitatively reproduce all features of the data. In the peripheral collisions, the interpretation of ρ_2 in terms of initial momentum anisotropy is complicated by possible residual nonflow and centrality fluctuations. In the mid-central collisions, the IP-Glasma + MUSIC model overestimates the ρ_2 and ρ_3 values in data, while other models underestimate them. In the central collisions, most models show good agreement with the ρ_2 values in data. A comparison of the ratio $\rho_{2,\mathrm{XeXe}}/\rho_{2,\mathrm{PbPb}}$ with the Trento model implies that the ^{129}Xe nucleus is a highly deformed triaxial ellipsoid, corresponding to a triaxiality value of $\gamma \approx 30^{\circ}$. This provides strong evidence of triaxial deformation of the ^{129}Xe nucleus using high-energy heavy-ion collisions.

ACKNOWLEDGMENTS

We thank CERN for the very successful operation of the LHC, as well as the support staff from our institutions without whom ATLAS could not be operated efficiently. We acknowledge the support of ANPCyT, Argentina; YerPhI, Armenia; ARC, Australia; BMWFW and FWF, Austria; ANAS, Azerbaijan; CNPq and FAPESP, Brazil; NSERC, NRC, and CFI, Canada; CERN; ANID, Chile; CAS, MOST, and NSFC, China; Minciencias, Colombia; MEYS CR, Czech Republic; DNRF and DNSRC, Denmark; IN2P3-CNRS and CEA-DRF/IRFU, France; SRNSFG, Georgia; BMBF, HGF and MPG, Germany; GSRI, Greece; RGC and Hong Kong SAR, China; ISF and Benoziyo Center, Israel; INFN, Italy; MEXT and JSPS, Japan; CNRST, Morocco; NWO, Netherlands; RCN, Norway; MEiN, Poland; FCT, Portugal; MNE/IFA, Romania; MESTD, Serbia; MSSR, Slovakia; ARRS and MIZŠ, Slovenia; DSI/NRF, South Africa; MICINN, Spain; SRC and Wallenberg Foundation, Sweden; SERI, SNSF, and Cantons of Bern and Geneva, Switzerland; MOST, Taiwan; TENMAK, Türkiye; STFC, United Kingdom; DOE and NSF, United States of America. In addition, individual groups and members have received support from BCKDF, CANARIE, Compute Canada, and CRC, Canada; PRIMUS 21/SCI/017 and UNCE SCI/013, Czech Republic; COST, ERC, ERDF, Horizon 2020, and Marie Skłodowska-Curie Actions, European Union; Investissements d'Avenir Labex, Investissements d'Avenir Idex, and ANR, France; DFG and AvH Foundation, Germany; Herakleitos, Thales, and Aristeia programs co-financed by EU-ESF and the Greek NSRF, Greece; BSF-NSF and MINERVA, Israel; Norwegian Financial Mechanism 2014-2021, Norway; NCN and NAWA, Poland; La Caixa Banking Foundation, CERCA Programme Generalitat de Catalunya, and PROMETEO and GenT Programmes Generalitat Valenciana, Spain; Göran Gustafssons Stiftelse, Sweden; The Royal Society and Leverhulme Trust, United Kingdom. The crucial computing support from all WLCG partners is acknowledged gratefully, in particular from CERN, the ATLAS Tier-1 facilities at TRIUMF (Canada), NDGF (Denmark, Norway, Sweden), CC-IN2P3 (France), KIT/GridKA (Germany), INFN-CNAF (Italy), NL-T1 (Netherlands), PIC (Spain), ASGC (Taiwan), RAL (UK), and BNL (USA), the Tier-2 facilities worldwide, and large non-WLCG resource providers. Major contributors of computing resources are listed in Ref. [79].

[1] C. Gale, S. Jeon, and B. Schenke, Hydrodynamic modeling of heavy-ion collisions, Int. J. Mod. Phys. A **28**, 1340011 (2013).

[2] U. Heinz and R. Snellings, Collective flow and viscosity in relativistic heavy-ion collisions, Annu. Rev. Nucl. Part. Sci. **63**, 123 (2013).

[3] P. Romatschke and U. Romatschke, *Relativistic Fluid Dynamics In and Out of Equilibrium*, Cambridge Monographs on Mathematical Physics (Cambridge University Press, Cambridge, 2019).

[4] F. G. Gardim, F. Grassi, M. Luzum, and J.-Y. Ollitrault, Mapping the hydrodynamic response to the initial geometry in heavy-ion collisions, Phys. Rev. C **85**, 024908 (2012).

[5] C. Gale, S. Jeon, B. Schenke, P. Tribedy, and R. Venugopalan, Event-by-Event Anisotropic Flow in Heavy-ion Collisions from Combined Yang-Mills and Viscous Fluid Dynamics, Phys. Rev. Lett. **110**, 012302 (2013).

[6] D. Teaney and L. Yan, Triangularity and dipole asymmetry in relativistic heavy ion collisions, Phys. Rev. C **83**, 064904 (2011).

[7] H. Niemi, G. S. Denicol, H. Holopainen, and P. Huovinen, Event-by-event distributions of azimuthal asymmetries in ultrarelativistic heavy-ion collisions, Phys. Rev. C **87**, 054901 (2013).

[8] A. Adare *et al.* (PHENIX Collaboration), Measurements of Higher-Order Flow Harmonics in Au+Au Collisions at $\sqrt{s_{NN}} =$ 200 GeV, Phys. Rev. Lett. **107**, 252301 (2011).

[9] K. Aamodt *et al.* (ALICE Collaboration), Higher Harmonic Anisotropic Flow Measurements of Charged Particles in Pb-Pb Collisions at $\sqrt{s_{NN}} = 2.76$ TeV, Phys. Rev. Lett. **107**, 032301 (2011).

[10] G. Aad *et al.* (ATLAS Collaboration), Measurement of the azimuthal anisotropy for charged particle production in $\sqrt{s_{NN}} =$ 2.76 TeV lead-lead collisions with the ATLAS detector, Phys. Rev. C **86**, 014907 (2012).

[11] S. Chatrchyan *et al.* (CMS Collaboration), Measurement of higher-order harmonic azimuthal anisotropy in PbPb collisions at $\sqrt{s_{NN}} = 2.76$ TeV, Phys. Rev. C **89**, 044906 (2014).

[12] G. Aad *et al.* (ATLAS Collaboration), Measurement of the distributions of event-by-event flow harmonics in lead-lead collisions at $\sqrt{s_{\rm NN}} = 2.76$ TeV with the ATLAS detector at the LHC, J. High Energy Phys. 11 (2013) 183.

[13] G. Aad *et al.* (ATLAS Collaboration), Measurement of event-plane correlations in $\sqrt{s_{NN}} = 2.76$ TeV lead-lead collisions with the ATLAS detector, Phys. Rev. C **90**, 024905 (2014).

[14] G. Aad *et al.* (ATLAS Collaboration), Measurement of the correlation between flow harmonics of different order in lead-lead collisions at $\sqrt{s_{NN}} = 2.76$ TeV with the ATLAS detector, Phys. Rev. C **92**, 034903 (2015).

[15] M. Luzum and J.-Y. Ollitrault, Extracting the shear viscosity of the quark-gluon plasma from flow in ultra-central heavy-ion collisions, Nucl. Phys. A **904-905**, 377c (2013).

[16] Z. Qiu and U. Heinz, Hydrodynamic event-plane correlations in Pb+Pb collisions at $\sqrt{s} = 2.76\,A$TeV, Phys. Lett. B **717**, 261 (2012).

[17] D. Teaney and L. Yan, Event-plane correlations and hydrodynamic simulations of heavy ion collisions, Phys. Rev. C **90**, 024902 (2014).

[18] P. Bożek and W. Broniowski, Transverse-momentum fluctuations in relativistic heavy-ion collisions from event-by-event viscous hydrodynamics, Phys. Rev. C **85**, 044910 (2012).

[19] P. Bozek, W. Broniowski, and S. Chatterjee, Transverse momentum fluctuations and correlations, Acta Phys. Pol. B Proc. Suppl. **10**, 1091 (2017).

[20] P. Bożek, Transverse-momentum-flow correlations in relativistic heavy-ion collisions, Phys. Rev. C **93**, 044908 (2016).

[21] B. Schenke, C. Shen, and D. Teaney, Transverse momentum fluctuations and their correlation with elliptic flow in nuclear collision, Phys. Rev. C **102**, 034905 (2020).

[22] G. Giacalone, B. Schenke, and C. Shen, Observable Signatures of Initial State Momentum Anisotropies in Nuclear Collisions, Phys. Rev. Lett. **125**, 192301 (2020).

[23] G. Giacalone, B. Schenke, and C. Shen, Constraining the Nucleon Size with Relativistic Nuclear Collisions, Phys. Rev. Lett. **128**, 042301 (2022).

[24] G. Aad *et al.* (ATLAS Collaboration), Measurement of flow harmonics correlations with mean transverse momentum in lead-lead and proton-lead collisions at $\sqrt{s_{NN}} = 5.02$ TeV with the ATLAS detector, Eur. Phys. J. C **79**, 985 (2019).

[25] S. Acharya *et al.* (ALICE Collaboration), Characterizing the initial conditions of heavy-ion collisions at the LHC with mean transverse momentum and anisotropic flow correlations, Phys. Lett. B **834**, 137393 (2022).

[26] G. Giacalone, F. G. Gardim, J. Noronha-Hostler and J.-Y. Ollitrault, Correlation between mean transverse momentum and anisotropic flow in heavy-ion collisions, Phys. Rev. C **103**, 024909 (2021).

[27] G. Giacalone, Observing the Deformation of Nuclei with Relativistic Nuclear Collisions, Phys. Rev. Lett. **124**, 202301 (2020).

[28] G. Giacalone, Constraining the quadrupole deformation of atomic nuclei with relativistic nuclear collisions, Phys. Rev. C **102**, 024901 (2020).

[29] J. Jia, Shape of atomic nuclei in heavy ion collisions, Phys. Rev. C **105**, 014905 (2022).

[30] J. Jia, S. Huang, and C. Zhang, Probing nuclear quadrupole deformation from correlation of elliptic flow and transverse momentum in heavy ion collisions, Phys. Rev. C **105**, 014906 (2022).

[31] B. Bally, M. Bender, G. Giacalone, and V. Soma, Evidence of the Triaxial Structure of ^{129}Xe at the Large Hadron Collider, Phys. Rev. Lett. **128**, 082301 (2022).

[32] J. Jia, Probing triaxial deformation of atomic nuclei in high-energy heavy ion collisions, Phys. Rev. C **105**, 044905 (2022).

[33] *Nuclear Structure*, edited by A. Bohr and B. R. Mottelson (World Scientific, Singapore, 1998).

[34] P. Moller, A. J. Sierk, T. Ichikawa, and H. Sagawa, Nuclear ground-state masses and deformations: FRDM (2012), At. Data Nucl. Data Tables **109-110**, 1 (2016).

[35] S. Raman, C. W. Nestor, Jr., and P. Tikkanen, Transition probability from the ground to the first-excited 2^+ state of even-even nuclides, At. Data Nucl. Data Tables **78**, 1 (2001).

[36] G. Giacalone, Elliptic flow fluctuations in central collisions of spherical and deformed nuclei, Phys. Rev. C **99**, 024910 (2019).

[37] ALICE Collaboration, Anisotropic flow in Xe-Xe collisions at $\sqrt{s_{\rm NN}} = 5.44$ TeV, Phys. Lett. B **784**, 82 (2018).

[38] S. Acharya *et al.* (CMS Collaboration), Charged-particle angular correlations in XeXe collisions at $\sqrt{s_{NN}} = 5.44$ TeV, Phys. Rev. C **100**, 044902 (2019).

[39] G. Aad *et al.* (ATLAS Collaboration), Measurement of the azimuthal anisotropy of charged-particle production in Xe+Xe collisions at $\sqrt{s_{NN}} = 5.44$ TeV with the ATLAS detector, Phys. Rev. C **101**, 024906 (2020).

[40] J. Jia, M. Zhou, and A. Trzupek, Revealing long-range multiparticle collectivity in small collision systems via subevent cumulants, Phys. Rev. C **96**, 034906 (2017).

[41] P. Huo, K. Gajdošová, J. Jia, and Y. Zhou, Importance of non-flow in mixed-harmonic multi-particle correlations in small collision systems, Phys. Lett. B **777**, 201 (2018).

[42] V. Skokov, B. Friman, and K. Redlich, Volume fluctuations and higher order cumulants of the net baryon number, Phys. Rev. C **88**, 034911 (2013).

[43] X. Luo, J. Xu, B. Mohanty, and N. Xu, Volume fluctuation and auto-correlation effects in the moment analysis of net-proton multiplicity distributions in heavy-ion collisions, J. Phys. G **40**, 105104 (2013).

[44] M. Zhou and J. Jia, Centrality fluctuations in heavy-ion collisions, Phys. Rev. C **98**, 044903 (2018).

[45] M. Aaboud *et al.* (ATLAS Collaboration), Fluctuations of anisotropic flow in Pb+Pb collisions at $\sqrt{s_{\rm NN}} = 5.02$ TeV with the ATLAS detector, J. High Energy Phys. 01 (2020) 051.

[46] P. Bożek and H. Mehrabpour, Correlation coefficient between harmonic flow and transverse momentum in heavy-ion collisions, Phys. Rev. C **101**, 064902 (2020).

[47] J. Jia, C. Zhang, and J. Xu, Centrality fluctuations and decorrelations in heavy-ion collisions in a Glauber model, Phys. Rev. Res. **2**, 023319 (2020).

[48] K. V. Yousefnia, A. Kotibhaskar, R. Bhalerao, and J.-Y. Ollitrault, Bayesian approach to long-range correlations and multiplicity fluctuations in nucleus-nucleus collisions, Phys. Rev. C **105**, 014907 (2022).

[49] G. Aad *et al.* (ATLAS Collaboration), The ATLAS Experiment at the CERN Large Hadron Collider, J. Instrum. **3**, S08003 (2008).

[50] ATLAS Collaboration, The ATLAS Collaboration Software and Firmware, CERN Report No. ATL-SOFT-PUB-2021-001, 2021 (unpublished), https://cds.cern.ch/record/2767187.

[51] M. Aaboud *et al.* (ATLAS Collaboration), Performance of the ATLAS trigger system in 2015, Eur. Phys. J. C **77**, 317 (2017).

[52] M. L. Miller, K. Reygers, S. J. Sanders, and P. Steinberg, Glauber modeling in high-energy nuclear collisions, Annu. Rev. Nucl. Part. Sci. **57**, 205 (2007).

[53] G. Aad *et al.* (ATLAS Collaboration), Measurement of the centrality dependence of the charged particle pseudorapidity distribution in lead-lead collisions at $\sqrt{s_{NN}} = 2.76$ TeV with the ATLAS detector, Phys. Lett. B **710**, 363 (2012).

[54] G. Aad *et al.* (ATLAS Collaboration), Z boson production in Pb+Pb collisions at $\sqrt{s_{\rm NN}} = 5.02$ TeV measured by the ATLAS experiment, Phys. Lett. B **802**, 135262 (2020).

[55] G. Aad *et al.* (ATLAS Collaboration), Measurement of charged-particle spectra in Pb+Pb collisions at $\sqrt{s_{\rm NN}} = 2.76$ TeV with the ATLAS detector at the LHC, J. High Energy Phys. 09 (2015) 050.

[56] G. Aad *et al.* (ATLAS Collaboration), Measurement of the pseudorapidity and transverse momentum dependence of the elliptic flow of charged particles in lead-lead collisions at $\sqrt{s_{NN}} =$ 2.76 TeV with the ATLAS detector, Phys. Lett. B **707**, 330 (2012).

[57] ATLAS Collaboration, Determination of secondary tracks in the minimum bias with charged tracks analysis at $\sqrt{(s)} = 900$ GeV, CERN Report No. ATL-INDET-INT-2010-017, 2010 (unpublished), https://cds.cern.ch/record/1297225.

[58] M. Gyulassy and X.-N. Wang, H. ING 1.0: A Monte Carlo program for parton and particle production in high-energy hadronic and nuclear collisions, Comput. Phys. Commun. **83**, 307 (1994).

[59] M. Masera, G. Ortona, M. G. Poghosyan, and F. Prino, Anisotropic transverse flow introduction in Monte Carlo generators for heavy ion collisions, Phys. Rev. C **79**, 064909 (2009).

[60] S. Agostinelli *et al.*, GEANT4 – a simulation toolkit, Nucl. Instrum. Methods Phys. Res., Sect. A **506**, 250 (2003).

[61] G. Aad *et al.* (ATLAS Collaboration), The ATLAS Simulation Infrastructure, Eur. Phys. J. C **70**, 823 (2010).

[62] G. Aad *et al.* (ATLAS Collaboration), Measurement of flow harmonics with multi-particle cumulants in Pb+Pb collisions at $\sqrt{s_{\rm NN}} = 2.76$ TeV with the ATLAS detector, Eur. Phys. J. C **74**, 3157 (2014).

[63] A. Bilandzic, R. Snellings, and S. Voloshin, Flow analysis with cumulants: Direct calculations, Phys. Rev. C **83**, 044913 (2011).

[64] A. Bilandzic, C. H. Christensen, K. Gulbrandsen, A. Hansen, and Y. Zhou, Generic framework for anisotropic flow analyses with multiparticle azimuthal correlations, Phys. Rev. C **89**, 064904 (2014).

[65] C. Zhang, A. Behera, S. Bhatta, and J. Jia, Non-flow effects in correlation between harmonic flow and transverse momentum in nuclear collisions, Phys. Lett. B **822**, 136702 (2021).

[66] B. Efron, Bootstrap methods: Another look at the jackknife, Ann. Stat. **7**, 1 (1979).

[67] ATLAS Collaboration, Evaluating statistical uncertainties and correlations using the bootstrap method, CERN Report No. ATL-PHYS-PUB-2021-011, 2021 (unpublished), https://cds.cern.ch/record/2759945.

[68] N. Borghini, P. M. Dinh, and J.-Y. Ollitrault, A New method for measuring azimuthal distributions in nucleus-nucleus collisions, Phys. Rev. C **63**, 054906 (2001).

[69] M. Aaboud *et al.* (ATLAS Collaboration), Measurement of long-range multiparticle azimuthal correlations with the subevent cumulant method in pp and $p+$Pb collisions with the ATLAS detector at the CERN Large Hadron Collider, Phys. Rev. C **97**, 024904 (2018).

[70] M. Aaboud *et al.* (ATLAS Collaboration), Measurement of multi-particle azimuthal correlations in pp, $p+$Pb and low-multiplicity Pb + Pb collisions with the ATLAS detector, Eur. Phys. J. C **77**, 428 (2017).

[71] M. Aaboud *et al.* (ATLAS Collaboration), Measurement of the azimuthal anisotropy of charged particles produced in $\sqrt{s_{\rm NN}} =$ 5.02 TeV Pb+Pb collisions with the ATLAS detector, Eur. Phys. J. C **78**, 997 (2018).

[72] J. Jia and P. Huo, Forward-backward eccentricity and participant-plane angle fluctuations and their influences on longitudinal dynamics of collective flow, Phys. Rev. C **90**, 034915 (2014).

[73] L.-G. Pang, H. Petersen, G.-Y. Qin, V. Roy, and X.-N. Wang, Decorrelation of anisotropic flow along the longitudinal direction, Eur. Phys. J. A **52**, 97 (2016).

[74] S. H. Lim and J. L. Nagle, Exploring origins for correlations between flow harmonics and transverse momentum in small collision systems, Phys. Rev. C **103**, 064906 (2021).

[75] J. S. Moreland, J. E. Bernhard, and S. A. Bass, Alternative ansatz to wounded nucleon and binary collision scaling in high-energy nuclear collisions, Phys. Rev. C **92**, 011901(R) (2015).

[76] G. Giacalone, A matter of shape: Seeing the deformation of atomic nuclei at high-energy colliders, arXiv:2101.00168.

[77] G. Nijs and W. van der Schee, Predictions and postdictions for relativistic lead and oxygen collisions with the computational simulation code Trajectum, Phys. Rev. C **106**, 044903 (2022).

[78] A. I. Budaca and R. Budaca, Triaxiality and state-dependent shape properties of Xe isotopes, Phys. Rev. C **101**, 064318 (2020).

[79] ATLAS Collaboration, ATLAS Computing Acknowledgements, CERN Report No. ATL-SOFT-PUB-2021-003, 2021 (unpublished), https://cds.cern.ch/record/2776662.

G. Aad,[101] B. Abbott,[119] D. C. Abbott,[102] K. Abeling,[55] S. H. Abidi,[29] A. Aboulhorma,[35e] H. Abramowicz,[150] H. Abreu,[149] Y. Abulaiti,[116] A. C. Abusleme Hoffman,[136a] B. S. Acharya,[68a,68b,a] B. Achkar,[55] L. Adam,[99] C. Adam Bourdarios,[4] L. Adamczyk,[84a] L. Adamek,[154] S. V. Addepalli,[26] J. Adelman,[114] A. Adiguzel,[21c] S. Adorni,[56] T. Adye,[133] A. A. Affolder,[135] Y. Afik,[36] M. N. Agaras,[13] J. Agarwala,[72a,72b] A. Aggarwal,[99] C. Agheorghiesei,[27c] J. A. Aguilar-Saavedra,[129f] A. Ahmad,[36] F. Ahmadov,[38,b] W. S. Ahmed,[103] X. Ai,[48] G. Aielli,[75a,75b] I. Aizenberg,[167] M. Akbiyik,[99] T. P. A. Åkesson,[97] A. V. Akimov,[37] K. Al Khoury,[41] G. L. Alberghi,[23b] J. Albert,[163] P. Albicocco,[53] M. J. Alconada Verzini,[89] S. Alderweireldt,[52] M. Aleksa,[36] I. N. Aleksandrov,[38] C. Alexa,[27b] T. Alexopoulos,[10] A. Alfonsi,[113] F. Alfonsi,[23b] M. Alhroob,[119] B. Ali,[131] S. Ali,[147] M. Aliev,[37] G. Alimonti,[70a] C. Allaire,[36] B. M. M. Allbrooke,[145] P. P. Allport,[20] A. Aloisio,[71a,71b]

F. Alonso,[89] C. Alpigiani,[137] E. Alunno Camelia,[75a,75b] M. Alvarez Estevez,[98] M. G. Alviggi,[71a,71b] Y. Amaral Coutinho,[81b] A. Ambler,[103] C. Amelung,[36] C. G. Ames,[108] D. Amidei,[105] S. P. Amor Dos Santos,[129a] S. Amoroso,[48] K. R. Amos,[161] C. S. Amrouche,[56] V. Ananiev,[124] C. Anastopoulos,[138] N. Andari,[134] T. Andeen,[11] J. K. Anders,[19] S. Y. Andrean,[47a,47b] A. Andreazza,[70a,70b] S. Angelidakis,[9] A. Angerami,[41,c] A. V. Anisenkov,[37] A. Annovi,[73a] C. Antel,[56] M. T. Anthony,[138] E. Antipov,[120] M. Antonelli,[53] D. J. A. Antrim,[17a] F. Anulli,[74a] M. Aoki,[82] J. A. Aparisi Pozo,[161] M. A. Aparo,[145] L. Aperio Bella,[48] C. Appelt,[18] N. Aranzabal,[36] V. Araujo Ferraz,[81a] C. Arcangeletti,[53] A. T. H. Arce,[51] E. Arena,[91] J.-F. Arguin,[107] S. Argyropoulos,[54] J.-H. Arling,[48] A. J. Armbruster,[36] O. Arnaez,[154] H. Arnold,[113] Z. P. Arrubarrena Tame,[108] G. Artoni,[74a,74b] H. Asada,[110] K. Asai,[117] S. Asai,[152] N. A. Asbah,[61] E. M. Asimakopoulou,[159] J. Assahsah,[35d] K. Assamagan,[29] R. Astalos,[28a] R. J. Atkin,[33a] M. Atkinson,[160] N. B. Atlay,[18] H. Atmani,[62b] P. A. Atmasiddha,[105] K. Augsten,[131] S. Auricchio,[71a,71b] A. D. Auriol,[20] V. A. Austrup,[169] G. Avner,[149] G. Avolio,[36] K. Axiotis,[56] M. K. Ayoub,[14c] G. Azuelos,[107,d] D. Babal,[28a] H. Bachacou,[134] K. Bachas,[151,e] A. Bachiu,[34] F. Backman,[47a,47b] A. Badea,[61] P. Bagnaia,[74a,74b] M. Bahmani,[18] A. J. Bailey,[161] V. R. Bailey,[160] J. T. Baines,[133] C. Bakalis,[10] O. K. Baker,[170] P. J. Bakker,[113] E. Bakos,[15] D. Bakshi Gupta,[8] S. Balaji,[146] R. Balasubramanian,[113] E. M. Baldin,[37] P. Balek,[132] E. Ballabene,[70a,70b] F. Balli,[134] L. M. Baltes,[63a] W. K. Balunas,[32] J. Balz,[99] E. Banas,[85] M. Bandieramonte,[128] A. Bandyopadhyay,[24] S. Bansal,[24] L. Barak,[150] E. L. Barberio,[104] D. Barberis,[57b,57a] M. Barbero,[101] G. Barbour,[95] K. N. Barends,[33a] T. Barillari,[109] M-S. Barisits,[36] J. Barkeloo,[122] T. Barklow,[142] R. M. Barnett,[17a] P. Baron,[121] D. A. Baron Moreno,[100] A. Baroncelli,[62a] G. Barone,[29] A. J. Barr,[125] L. Barranco Navarro,[47a,47b] F. Barreiro,[98] J. Barreiro Guimarães da Costa,[14a] U. Barron,[150] M. G. Barros Teixeira,[129a] S. Barsov,[37] F. Bartels,[63a] R. Bartoldus,[142] A. E. Barton,[90] P. Bartos,[28a] A. Basalaev,[48] A. Basan,[99] M. Baselga,[49] I. Bashta,[76a,76b] A. Bassalat,[66,f] M. J. Basso,[154] C. R. Basson,[100] R. L. Bates,[59] S. Batlamous,[35e] J. R. Batley,[32] B. Batool,[140] M. Battaglia,[135] M. Bauce,[74a,74b] P. Bauer,[24] A. Bayirli,[21a] J. B. Beacham,[51] T. Beau,[126] P. H. Beauchemin,[157] F. Becherer,[54] P. Bechtle,[24] H. P. Beck,[19,g] K. Becker,[165] C. Becot,[48] A. J. Beddall,[21d] V. A. Bednyakov,[38] C. P. Bee,[144] L. J. Beemster,[15] T. A. Beermann,[36] M. Begalli,[81b,81d] M. Begel,[29] A. Behera,[144] J. K. Behr,[48] C. Beirao Da Cruz E Silva,[36] J. F. Beirer,[55,36] F. Beisiegel,[24] M. Belfkir,[115b] G. Bella,[150] L. Bellagamba,[23b] A. Bellerive,[34] P. Bellos,[20] K. Beloborodov,[37] K. Belotskiy,[37] N. L. Belyaev,[37] D. Benchekroun,[35a] F. Bendebba,[35a] Y. Benhammou,[150] D. P. Benjamin,[29] M. Benoit,[29] J. R. Bensinger,[26] S. Bentvelsen,[113] L. Beresford,[36] M. Beretta,[53] D. Berge,[18] E. Bergeaas Kuutmann,[159] N. Berger,[4] B. Bergmann,[131] J. Beringer,[17a] S. Berlendis,[7] G. Bernardi,[5] C. Bernius,[142] F. U. Bernlochner,[24] T. Berry,[94] P. Berta,[132] A. Berthold,[50] I. A. Bertram,[90] O. Bessidskaia Bylund,[169] S. Bethke,[109] A. Betti,[44] A. J. Bevan,[93] M. Bhamjee,[33c] S. Bhatta,[144] D. S. Bhattacharya,[164] P. Bhattarai,[26] V. S. Bhopatkar,[6] R. Bi,[128] R. Bi,[29,s] R. M. Bianchi,[128] O. Biebel,[108] R. Bielski,[122] N. V. Biesuz,[73a,73b] M. Biglietti,[76a] T. R. V. Billoud,[131] M. Bindi,[55] A. Bingul,[21b] C. Bini,[74a,74b] S. Biondi,[23b,23a] A. Biondini,[91] C. J. Birch-sykes,[100] G. A. Bird,[20,133] M. Birman,[167] T. Bisanz,[36] D. Biswas,[168,h] A. Bitadze,[100] K. Bjørke,[124] I. Bloch,[48] C. Blocker,[26] A. Blue,[59] U. Blumenschein,[93] J. Blumenthal,[99] G. J. Bobbink,[113] V. S. Bobrovnikov,[37] M. Boehler,[54] D. Bogavac,[36] A. G. Bogdanchikov,[37] C. Bohm,[47a] V. Boisvert,[94] P. Bokan,[48] T. Bold,[84a] M. Bomben,[5] M. Bona,[93] M. Boonekamp,[134] C. D. Booth,[94] A. G. Borbély,[59] H. M. Borecka-Bielska,[107] L. S. Borgna,[95] G. Borissov,[90] D. Bortoletto,[125] D. Boscherini,[23b] M. Bosman,[13] J. D. Bossio Sola,[36] K. Bouaouda,[35a] J. Boudreau,[128] E. V. Bouhova-Thacker,[90] D. Boumediene,[40] R. Bouquet,[5] A. Boveia,[118] J. Boyd,[36] D. Boye,[29] I. R. Boyko,[38] J. Bracinik,[20] N. Brahimi,[62d,62c] G. Brandt,[169] O. Brandt,[32] F. Braren,[48] B. Brau,[102] J. E. Brau,[122] W. D. Breaden Madden,[59] K. Brendlinger,[48] R. Brener,[167] L. Brenner,[36] R. Brenner,[159] S. Bressler,[167] B. Brickwedde,[99] D. Britton,[59] D. Britzger,[109] I. Brock,[24] G. Brooijmans,[41] W. K. Brooks,[136f] E. Brost,[29] P. A. Bruckman de Renstrom,[85] B. Brüers,[48] D. Bruncko,[28b,i] A. Bruni,[23b] G. Bruni,[23b] M. Bruschi,[23b] N. Bruscino,[74a,74b] L. Bryngemark,[142] T. Buanes,[16] Q. Buat,[137] P. Buchholz,[140] A. G. Buckley,[59] I. A. Budagov,[38,i] M. K. Bugge,[124] O. Bulekov,[37] B. A. Bullard,[61] S. Burdin,[91] C. D. Burgard,[48] A. M. Burger,[40] B. Burghgrave,[8] J. T. P. Burr,[32] C. D. Burton,[11] J. C. Burzynski,[141] E. L. Busch,[41] V. Büscher,[99] P. J. Bussey,[59] J. M. Butler,[25] C. M. Buttar,[59] J. M. Butterworth,[95] W. Buttinger,[133] C. J. Buxo Vazquez,[106] A. R. Buzykaev,[37] G. Cabras,[23b] S. Cabrera Urbán,[161] D. Caforio,[58] H. Cai,[128] Y. Cai,[14a,14d] V. M. M. Cairo,[36] O. Cakir,[3a] N. Calace,[36] P. Calafiura,[17a] G. Calderini,[126] P. Calfayan,[67] G. Callea,[59] L. P. Caloba,[81b] D. Calvet,[40] S. Calvet,[40] T. P. Calvet,[101] M. Calvetti,[73a,73b] R. Camacho Toro,[126] S. Camarda,[36] D. Camarero Munoz,[98] P. Camarri,[75a,75b] M. T. Camerlingo,[76a,76b] D. Cameron,[124] C. Camincher,[163] M. Campanelli,[95] A. Camplani,[42] V. Canale,[71a,71b] A. Canesse,[103] M. Cano Bret,[79] J. Cantero,[161] Y. Cao,[160] F. Capocasa,[26] M. Capua,[43b,43a] A. Carbone,[70a,70b] R. Cardarelli,[75a] J. C. J. Cardenas,[8] F. Cardillo,[161] T. Carli,[36] G. Carlino,[71a] B. T. Carlson,[128,j] E. M. Carlson,[163,155a] L. Carminati,[70a,70b] M. Carnesale,[74a,74b] S. Caron,[112] E. Carquin,[136f] S. Carrá,[70a,70b] G. Carratta,[23b,23a] F. Carrio Argos,[33g] J. W. S. Carter,[154] T. M. Carter,[52] M. P. Casado,[13,k] A. F. Casha,[154] E. G. Castiglia,[170] F. L. Castillo,[63a] L. Castillo Garcia,[13] V. Castillo Gimenez,[161] N. F. Castro,[129a,129e] A. Catinaccio,[36] J. R. Catmore,[124] V. Cavaliere,[29] N. Cavalli,[23b,23a] V. Cavasinni,[73a,73b] E. Celebi,[21a] F. Celli,[125] M. S. Centonze,[69a,69b] K. Cerny,[121] A. S. Cerqueira,[81a] A. Cerri,[145] L. Cerrito,[75a,75b] F. Cerutti,[17a] A. Cervelli,[23b] S. A. Cetin,[21d] Z. Chadi,[35a] D. Chakraborty,[114] M. Chala,[129f] J. Chan,[168]

W. S. Chan,[113] W. Y. Chan,[152] J. D. Chapman,[32] B. Chargeishvili,[148b] D. G. Charlton,[20] T. P. Charman,[93] M. Chatterjee,[19] S. Chekanov,[6] S. V. Chekulaev,[155a] G. A. Chelkov,[38,l] A. Chen,[105] B. Chen,[150] B. Chen,[163] C. Chen,[62a] H. Chen,[14c] H. Chen,[29] J. Chen,[62c] J. Chen,[26] S. Chen,[152] S. J. Chen,[14c] X. Chen,[62c] X. Chen,[14b,m] Y. Chen,[62a] C. L. Cheng,[168] H. C. Cheng,[64a] A. Cheplakov,[38] E. Cheremushkina,[48] E. Cherepanova,[113] R. Cherkaoui El Moursli,[35e] E. Cheu,[7] K. Cheung,[65] L. Chevalier,[134] V. Chiarella,[53] G. Chiarelli,[73a] G. Chiodini,[69a] A. S. Chisholm,[20] A. Chitan,[27b] Y. H. Chiu,[163] M. V. Chizhov,[38] K. Choi,[11] A. R. Chomont,[74a,74b] Y. Chou,[102] E. Y. S. Chow,[113] T. Chowdhury,[33g] L. D. Christopher,[33g] K. L. Chu,[64a] M. C. Chu,[64a] X. Chu,[14a,14d] J. Chudoba,[130] J. J. Chwastowski,[85] D. Cieri,[109] K. M. Ciesla,[84a] V. Cindro,[92] A. Ciocio,[17a] F. Cirotto,[71a,71b] Z. H. Citron,[167,n] M. Citterio,[70a] D. A. Ciubotaru,[27b] B. M. Ciungu,[154] A. Clark,[56] P. J. Clark,[52] J. M. Clavijo Columbie,[48] S. E. Clawson,[100] C. Clement,[47a,47b] J. Clercx,[48] L. Clissa,[23b,23a] Y. Coadou,[101] M. Cobal,[68a,68c] A. Coccaro,[57b] R. F. Coelho Barrue,[129a] R. Coelho Lopes De Sa,[102] S. Coelli,[70a] H. Cohen,[150] A. E. C. Coimbra,[70a,70b] B. Cole,[41] J. Collot,[60] P. Conde Muiño,[129a,129g] S. H. Connell,[33c] I. A. Connelly,[59] E. I. Conroy,[125] F. Conventi,[71a,o] H. G. Cooke,[20] A. M. Cooper-Sarkar,[125] F. Cormier,[162] L. D. Corpe,[36] M. Corradi,[74a,74b] E. E. Corrigan,[97] F. Corriveau,[103,p] A. Cortes-Gonzalez,[18] M. J. Costa,[161] F. Costanza,[4] D. Costanzo,[138] B. M. Cote,[118] G. Cowan,[94] J. W. Cowley,[32] K. Cranmer,[116] S. Crépé-Renaudin,[60] F. Crescioli,[126] M. Cristinziani,[140] M. Cristoforetti,[77a,77b,q] V. Croft,[157] G. Crosetti,[43b,43a] A. Cueto,[36] T. Cuhadar Donszelmann,[158] H. Cui,[14a,14d] Z. Cui,[7] A. R. Cukierman,[142] W. R. Cunningham,[59] F. Curcio,[43b,43a] P. Czodrowski,[36] M. M. Czurylo,[63b] M. J. Da Cunha Sargedas De Sousa,[62a] J. V. Da Fonseca Pinto,[81b] C. Da Via,[100] W. Dabrowski,[84a] T. Dado,[49] S. Dahbi,[33g] T. Dai,[105] C. Dallapiccola,[102] M. Dam,[42] G. D'amen,[29] V. D'Amico,[76a,76b] J. Damp,[99] J. R. Dandoy,[127] M. F. Daneri,[30] M. Danninger,[141] V. Dao,[36] G. Darbo,[57b] S. Darmora,[6] S. J. Das,[29] A. Dattagupta,[122] S. D'Auria,[70a,70b] C. David,[155b] T. Davidek,[132] D. R. Davis,[51] B. Davis-Purcell,[34] I. Dawson,[93] K. De,[8] R. De Asmundis,[71a] M. De Beurs,[113] S. De Castro,[23b,23a] N. De Groot,[112] P. de Jong,[113] H. De la Torre,[106] A. De Maria,[14c] A. De Salvo,[74a] U. De Sanctis,[75a,75b] M. De Santis,[75a,75b] A. De Santo,[145] J. B. De Vivie De Regie,[60] D. V. Dedovich,[38] J. Degens,[113] A. M. Deiana,[44] F. Del Corso,[23b,23a] J. Del Peso,[98] F. Del Rio,[63a] F. Deliot,[134] C. M. Delitzsch,[49] M. Della Pietra,[71a,71b] D. Della Volpe,[56] A. Dell'Acqua,[36] L. Dell'Asta,[70a,70b] M. Delmastro,[4] P. A. Delsart,[60] S. Demers,[170] M. Demichev,[38] S. P. Denisov,[37] L. D'Eramo,[114] D. Derendarz,[85] F. Derue,[126] P. Dervan,[91] K. Desch,[24] K. Dette,[154] C. Deutsch,[24] P. O. Deviveiros,[36] F. A. Di Bello,[74a,74b] A. Di Ciaccio,[75a,75b] L. Di Ciaccio,[4] A. Di Domenico,[74a,74b] C. Di Donato,[71a,71b] A. Di Girolamo,[36] G. Di Gregorio,[73a,73b] A. Di Luca,[77a,77b] B. Di Micco,[76a,76b] R. Di Nardo,[76a,76b] C. Diaconu,[101] F. A. Dias,[113] T. Dias Do Vale,[141] M. A. Diaz,[136a,136b] F. G. Diaz Capriles,[24] M. Didenko,[161] E. B. Diehl,[105] L. Diehl,[54] S. Díez Cornell,[48] C. Diez Pardos,[140] C. Dimitriadi,[24,159] A. Dimitrievska,[17a] W. Ding,[14b] J. Dingfelder,[24] I-M. Dinu,[27b] S. J. Dittmeier,[63b] F. Dittus,[36] F. Djama,[101] T. Djobava,[148b] J. I. Djuvsland,[16] D. Dodsworth,[26] C. Doglioni,[100,97] J. Dolejsi,[132] Z. Dolezal,[132] M. Donadelli,[81c] B. Dong,[62c] J. Donini,[40] A. D'Onofrio,[14c] M. D'Onofrio,[91] J. Dopke,[133] A. Doria,[71a] M. T. Dova,[89] A. T. Doyle,[59] M. A. Draguet,[125] E. Drechsler,[141] E. Dreyer,[167] I. Drivas-koulouris,[10] A. S. Drobac,[157] D. Du,[62a] T. A. du Pree,[113] F. Dubinin,[37] M. Dubovsky,[28a] E. Duchovni,[167] G. Duckeck,[108] O. A. Ducu,[36] D. Duda,[109] A. Dudarev,[36] M. D'uffizi,[100] L. Duflot,[66] M. Dührssen,[36] C. Dülsen,[169] A. E. Dumitriu,[27b] M. Dunford,[63a] S. Dungs,[49] K. Dunne,[47a,47b] A. Duperrin,[101] H. Duran Yildiz,[3a] M. Düren,[58] A. Durglishvili,[148b] B. L. Dwyer,[114] G. I. Dyckes,[17a] M. Dyndal,[84a] S. Dysch,[100] B. S. Dziedzic,[85] Z. O. Earnshaw,[145] B. Eckerova,[28a] M. G. Eggleston,[51] E. Egidio Purcino De Souza,[81b] L. F. Ehrke,[56] G. Eigen,[16] K. Einsweiler,[17a] T. Ekelof,[159] P. A. Ekman,[97] Y. El Ghazali,[35b] H. El Jarrari,[35e,147] A. El Moussaouy,[35a] V. Ellajosyula,[159] M. Ellert,[159] F. Ellinghaus,[169] A. A. Elliot,[93] N. Ellis,[36] J. Elmsheuser,[29] M. Elsing,[36] D. Emeliyanov,[133] A. Emerman,[41] Y. Enari,[152] I. Ene,[17a] S. Epari,[13] J. Erdmann,[49] A. Ereditato,[19] P. A. Erland,[85] M. Errenst,[169] M. Escalier,[66] C. Escobar,[161] E. Etzion,[150] G. Evans,[129a] H. Evans,[67] M. O. Evans,[145] A. Ezhilov,[37] S. Ezzarqtouni,[35a] F. Fabbri,[59] L. Fabbri,[23b,23a] G. Facini,[95] V. Fadeyev,[135] R. M. Fakhrutdinov,[37] S. Falciano,[74a] P. J. Falke,[24] S. Falke,[36] J. Faltova,[132] Y. Fan,[14a] Y. Fang,[14a,14d] G. Fanourakis,[46] M. Fanti,[70a,70b] M. Faraj,[68a,68b] A. Farbin,[8] A. Farilla,[76a] T. Farooque,[106] S. M. Farrington,[52] F. Fassi,[35e] D. Fassouliotis,[9] M. Faucci Giannelli,[75a,75b] W. J. Fawcett,[32] L. Fayard,[66] O. L. Fedin,[37,l] G. Fedotov,[37] M. Feickert,[160] L. Feligioni,[101] A. Fell,[138] D. E. Fellers,[122] C. Feng,[62b] M. Feng,[14b] M. J. Fenton,[158] A. B. Fenyuk,[37] L. Ferencz,[48] S. W. Ferguson,[45] J. A. Fernandez Pretel,[54] J. Ferrando,[48] A. Ferrari,[159] P. Ferrari,[113] R. Ferrari,[72a] D. Ferrere,[56] C. Ferretti,[105] F. Fiedler,[99] A. Filipčič,[92] E. K. Filmer,[1] F. Filthaut,[112] M. C. N. Fiolhais,[129a,129c,r] L. Fiorini,[161] F. Fischer,[140] W. C. Fisher,[106] T. Fitschen,[20,66] I. Fleck,[140] P. Fleischmann,[105] T. Flick,[169] L. Flores,[127] M. Flores,[33d] L. R. Flores Castillo,[64a] F. M. Follega,[77a,77b] N. Fomin,[16] J. H. Foo,[154] B. C. Forland,[67] A. Formica,[134] A. C. Forti,[100] E. Fortin,[101] A. W. Fortman,[61] M. G. Foti,[17a] L. Fountas,[9] D. Fournier,[66] H. Fox,[90] P. Francavilla,[73a,73b] S. Francescato,[61] M. Franchini,[23b,23a] S. Franchino,[63a] D. Francis,[36] L. Franco,[112] L. Franconi,[19] M. Franklin,[61] G. Frattari,[26] A. C. Freegard,[93] P. M. Freeman,[20] W. S. Freund,[81b] N. Fritzsche,[50] A. Froch,[54] D. Froidevaux,[36] J. A. Frost,[125] Y. Fu,[62a] M. Fujimoto,[117] E. Fullana Torregrosa,[161,i] J. Fuster,[161] A. Gabrielli,[23b,23a] A. Gabrielli,[36] P. Gadow,[48]

G. Gagliardi,[57b,57a] L. G. Gagnon,[17a] G. E. Gallardo,[125] E. J. Gallas,[125] B. J. Gallop,[133] R. Gamboa Goni,[93] K. K. Gan,[118] S. Ganguly,[152] J. Gao,[62a] Y. Gao,[52] F. M. Garay Walls,[136a,136b] B. Garcia,[29,s] C. García,[161] J. E. García Navarro,[161] J. A. García Pascual,[14a] M. Garcia-Sciveres,[17a] R. W. Gardner,[39] D. Garg,[79] R. B. Garg,[142] S. Gargiulo,[54] C. A. Garner,[154] V. Garonne,[29] S. J. Gasiorowski,[137] P. Gaspar,[81b] G. Gaudio,[72a] V. Gautam,[13] P. Gauzzi,[74a,74b] I. L. Gavrilenko,[37] A. Gavrilyuk,[37] C. Gay,[162] G. Gaycken,[48] E. N. Gazis,[10] A. A. Geanta,[27b] C. M. Gee,[135] J. Geisen,[97] M. Geisen,[99] C. Gemme,[57b] M. H. Genest,[60] S. Gentile,[74a,74b] S. George,[94] W. F. George,[20] T. Geralis,[46] L. O. Gerlach,[55] P. Gessinger-Befurt,[36] M. Ghasemi Bostanabad,[163] M. Ghneimat,[140] A. Ghosal,[140] A. Ghosh,[158] A. Ghosh,[7] B. Giacobbe,[23b] S. Giagu,[74a,74b] N. Giangiacomi,[154] P. Giannetti,[73a] A. Giannini,[62a] S. M. Gibson,[94] M. Gignac,[135] D. T. Gil,[84b] A. K. Gilbert,[84a] B. J. Gilbert,[41] D. Gillberg,[34] G. Gilles,[113] N. E. K. Gillwald,[48] L. Ginabat,[126] D. M. Gingrich,[2,d] M. P. Giordani,[68a,68c] P. F. Giraud,[134] G. Giugliarelli,[68a,68c] D. Giugni,[70a] F. Giuli,[36] I. Gkialas,[9,t] L. K. Gladilin,[37] C. Glasman,[98] G. R. Gledhill,[122] M. Glisic,[122] I. Gnesi,[43b,u] Y. Go,[29,s] M. Goblirsch-Kolb,[26] D. Godin,[107] S. Goldfarb,[104] T. Golling,[56] M. G. D. Gololo,[33g] D. Golubkov,[37] J. P. Gombas,[106] A. Gomes,[129a,129b] G. Gomes Da Silva,[140] A. J. Gomez Delegido,[161] R. Goncalves Gama,[55] R. Gonçalo,[129a,129c] G. Gonella,[122] L. Gonella,[20] A. Gongadze,[38] F. Gonnella,[20] J. L. Gonski,[41] S. González de la Hoz,[161] S. Gonzalez Fernandez,[13] R. Gonzalez Lopez,[91] C. Gonzalez Renteria,[17a] R. Gonzalez Suarez,[159] S. Gonzalez-Sevilla,[56] G. R. Gonzalvo Rodriguez,[161] R. Y. González Andana,[52] L. Goossens,[36] N. A. Gorasia,[20] P. A. Gorbounov,[37] B. Gorini,[36] E. Gorini,[69a,69b] A. Gorišek,[92] A. T. Goshaw,[51] M. I. Gostkin,[38] C. A. Gottardo,[112] M. Gouighri,[35b] V. Goumarre,[48] A. G. Goussiou,[137] N. Govender,[33c] C. Goy,[4] I. Grabowska-Bold,[84a] K. Graham,[34] E. Gramstad,[124] S. Grancagnolo,[18] M. Grandi,[145] V. Gratchev,[37] P. M. Gravila,[27f] F. G. Gravili,[69a,69b] H. M. Gray,[17a] M. Greco,[69a,69b] C. Grefe,[24] I. M. Gregor,[48] P. Grenier,[142] C. Grieco,[13] A. A. Grillo,[135] K. Grimm,[31,v] S. Grinstein,[13,w] J.-F. Grivaz,[66] E. Gross,[167] J. Grosse-Knetter,[55] C. Grud,[105] A. Grummer,[111] J. C. Grundy,[125] L. Guan,[105] W. Guan,[168] C. Gubbels,[162] J. G. R. Guerrero Rojas,[161] G. Guerrieri,[68a,68c] F. Guescini,[109] R. Gugel,[99] J. A. M. Guhit,[105] A. Guida,[48] T. Guillemin,[4] E. Guilloton,[165,133] S. Guindon,[36] F. Guo,[14a,14d] J. Guo,[62c] L. Guo,[66] Y. Guo,[105] R. Gupta,[48] S. Gurbuz,[24] S. S. Gurdasani,[54] G. Gustavino,[36] M. Guth,[56] P. Gutierrez,[119] L. F. Gutierrez Zagazeta,[127] C. Gutschow,[95] C. Guyot,[134] C. Gwenlan,[125] C. B. Gwilliam,[91] E. S. Haaland,[124] A. Haas,[116] M. Habedank,[48] C. Haber,[17a] H. K. Hadavand,[8] A. Hadef,[99] S. Hadzic,[109] M. Haleem,[164] J. Haley,[120] J. J. Hall,[138] G. D. Hallewell,[101] L. Halser,[19] K. Hamano,[163] H. Hamdaoui,[35e] M. Hamer,[24] G. N. Hamity,[52] J. Han,[62b] K. Han,[62a] L. Han,[14c] L. Han,[62a] S. Han,[17a] Y. F. Han,[154] K. Hanagaki,[82] M. Hance,[135] D. A. Hangal,[41,c] M. D. Hank,[39] R. Hankache,[100] J. B. Hansen,[42] J. D. Hansen,[42] P. H. Hansen,[42] K. Hara,[156] D. Harada,[56] T. Harenberg,[169] S. Harkusha,[37] Y. T. Harris,[125] P. F. Harrison,[165] N. M. Hartman,[142] N. M. Hartmann,[108] Y. Hasegawa,[139] A. Hasib,[52] S. Haug,[19] R. Hauser,[106] M. Havranek,[131] C. M. Hawkes,[20] R. J. Hawkings,[36] S. Hayashida,[110] D. Hayden,[106] C. Hayes,[105] R. L. Hayes,[162] C. P. Hays,[125] J. M. Hays,[93] H. S. Hayward,[91] F. He,[62a] Y. He,[153] Y. He,[126] M. P. Heath,[52] V. Hedberg,[97] A. L. Heggelund,[124] N. D. Hehir,[93] C. Heidegger,[54] K. K. Heidegger,[54] W. D. Heidorn,[80] J. Heilman,[34] S. Heim,[48] T. Heim,[17a] J. G. Heinlein,[127] J. J. Heinrich,[122] L. Heinrich,[36] J. Hejbal,[130] L. Helary,[48] A. Held,[116] S. Hellesund,[124] C. M. Helling,[162] S. Hellman,[47a,47b] C. Helsens,[36] R. C. W. Henderson,[90] L. Henkelmann,[32] A. M. Henriques Correia,[36] H. Herde,[142] Y. Hernández Jiménez,[144] H. Herr,[99] M. G. Herrmann,[108] T. Herrmann,[50] G. Herten,[54] R. Hertenberger,[108] L. Hervas,[36] N. P. Hessey,[155a] H. Hibi,[83] E. Higón-Rodriguez,[161] S. J. Hillier,[20] I. Hinchliffe,[17a] F. Hinterkeuser,[24] M. Hirose,[123] S. Hirose,[156] D. Hirschbuehl,[169] T. G. Hitchings,[100] B. Hiti,[92] J. Hobbs,[144] R. Hobincu,[27e] N. Hod,[167] M. C. Hodgkinson,[138] B. H. Hodkinson,[32] A. Hoecker,[36] J. Hofer,[48] D. Hohn,[54] T. Holm,[24] M. Holzbock,[109] L. B.A. H. Hommels,[32] B. P. Honan,[100] J. Hong,[62c] T. M. Hong,[128] Y. Hong,[55] J. C. Honig,[54] A. Hönle,[109] B. H. Hooberman,[160] W. H. Hopkins,[6] Y. Horii,[110] S. Hou,[147] A. S. Howard,[92] J. Howarth,[59] J. Hoya,[89] M. Hrabovsky,[121] A. Hrynevich,[37] T. Hryn'ova,[4] P. J. Hsu,[65] S.-C. Hsu,[137] Q. Hu,[41,c] Y. F. Hu,[14a,14d,x] D. P. Huang,[95] S. Huang,[64b] X. Huang,[14c] Y. Huang,[62a] Y. Huang,[14a] Z. Huang,[100] Z. Hubacek,[131] M. Huebner,[24] F. Huegging,[24] T. B. Huffman,[125] M. Huhtinen,[36] S. K. Huiberts,[16] R. Hulsken,[103] N. Huseynov,[12,l] J. Huston,[106] J. Huth,[61] R. Hyneman,[142] S. Hyrych,[28a] G. Iacobucci,[56] G. Iakovidis,[29] I. Ibragimov,[140] L. Iconomidou-Fayard,[66] P. Iengo,[71a,71b] R. Iguchi,[152] T. Iizawa,[56] Y. Ikegami,[82] A. Ilg,[19] N. Ilic,[154] H. Imam,[35a] T. Ingebretsen Carlson,[47a,47b] G. Introzzi,[72a,72b] M. Iodice,[76a] V. Ippolito,[74a,74b] M. Ishino,[152] W. Islam,[168] C. Issever,[18,48] S. Istin,[21a,y] H. Ito,[166] J. M. Iturbe Ponce,[64a] R. Iuppa,[77a,77b] A. Ivina,[167] J. M. Izen,[45] V. Izzo,[71a] P. Jacka,[130,131] P. Jackson,[1] R. M. Jacobs,[48] B. P. Jaeger,[141] C. S. Jagfeld,[108] G. Jäkel,[169] K. Jakobs,[54] T. Jakoubek,[167] J. Jamieson,[59] K. W. Janas,[84a] G. Jarlskog,[97] A. E. Jaspan,[91] T. Javůrek,[36] M. Javurkova,[102] F. Jeanneau,[134] L. Jeanty,[122] J. Jejelava,[148a,z] P. Jenni,[54,aa] C. E. Jessiman,[34] S. Jézéquel,[4] J. Jia,[144] X. Jia,[61] X. Jia,[14a,14d] Z. Jia,[14c] Y. Jiang,[62a] S. Jiggins,[52] J. Jimenez Pena,[109] S. Jin,[14c] A. Jinaru,[27b] O. Jinnouchi,[153] H. Jivan,[33g] P. Johansson,[138] K. A. Johns,[7] C. A. Johnson,[67] D. M. Jones,[32] E. Jones,[165] P. Jones,[32] R. W. L. Jones,[90] T. J. Jones,[91] J. Jovicevic,[15] X. Ju,[17a] J. J. Junggeburth,[36] A. Juste Rozas,[13,w] S. Kabana,[136e] A. Kaczmarska,[85] M. Kado,[74a,74b] H. Kagan,[118] M. Kagan,[142] A. Kahn,[41] A. Kahn,[127] C. Kahra,[99] T. Kaji,[166] E. Kajomovitz,[149] N. Kakati,[167] C. W. Kalderon,[29]

A. Kamenshchikov,[154] N. J. Kang,[135] Y. Kano,[110] D. Kar,[33g] K. Karava,[125] M. J. Kareem,[155b] E. Karentzos,[54] I. Karkanias,[151] S. N. Karpov,[38] Z. M. Karpova,[38] V. Kartvelishvili,[90] A. N. Karyukhin,[37] E. Kasimi,[151] C. Kato,[62d] J. Katzy,[48] S. Kaur,[34] K. Kawade,[139] K. Kawagoe,[88] T. Kawaguchi,[110] T. Kawamoto,[134] G. Kawamura,[55] E. F. Kay,[163] F. I. Kaya,[157] S. Kazakos,[13] V. F. Kazanin,[37] Y. Ke,[144] J. M. Keaveney,[33a] R. Keeler,[163] G. V. Kehris,[61] J. S. Keller,[34] A. S. Kelly,[95] D. Kelsey,[145] J. J. Kempster,[20] J. Kendrick,[20] K. E. Kennedy,[41] O. Kepka,[130] B. P. Kerridge,[165] S. Kersten,[169] B. P. Kerševan,[92] L. Keszeghova,[28a] S. Ketabchi Haghighat,[154] M. Khandoga,[126] A. Khanov,[120] A. G. Kharlamov,[37] T. Kharlamova,[37] E. E. Khoda,[137] T. J. Khoo,[18] G. Khoriauli,[164] J. Khubua,[148b] Y. A. R. Khwaira,[66] M. Kiehn,[36] A. Kilgallon,[122] D. W. Kim,[47a,47b] E. Kim,[153] Y. K. Kim,[39] N. Kimura,[95] A. Kirchhoff,[55] D. Kirchmeier,[50] C. Kirfel,[24] J. Kirk,[133] A. E. Kiryunin,[109] T. Kishimoto,[152] D. P. Kisliuk,[154] C. Kitsaki,[10] O. Kivernyk,[24] M. Klassen,[63a] C. Klein,[34] L. Klein,[164] M. H. Klein,[105] M. Klein,[91] U. Klein,[91] P. Klimek,[36] A. Klimentov,[29] F. Klimpel,[109] T. Klingl,[24] T. Klioutchnikova,[36] F. F. Klitzner,[108] P. Kluit,[113] S. Kluth,[109] E. Kneringer,[78] T. M. Knight,[154] A. Knue,[54] D. Kobayashi,[88] R. Kobayashi,[86] M. Kocian,[142] T. Kodama,[152] P. Kodyš,[132] D. M. Koeck,[145] P. T. Koenig,[24] T. Koffas,[34] N. M. Köhler,[36] M. Kolb,[134] I. Koletsou,[4] T. Komarek,[121] K. Köneke,[54] A. X. Y. Kong,[1] T. Kono,[117] N. Konstantinidis,[95] B. Konya,[97] R. Kopeliansky,[67] S. Koperny,[84a] K. Korcyl,[85] K. Kordas,[151] G. Koren,[150] A. Korn,[95] S. Korn,[55] I. Korolkov,[13] N. Korotkova,[37] B. Kortman,[113] O. Kortner,[109] S. Kortner,[109] W. H. Kostecka,[114] V. V. Kostyukhin,[140] A. Kotsokechagia,[66] A. Kotwal,[51] A. Koulouris,[36] A. Kourkoumeli-Charalampidi,[72a,72b] C. Kourkoumelis,[9] E. Kourlitis,[6] O. Kovanda,[145] R. Kowalewski,[163] W. Kozanecki,[134] A. S. Kozhin,[37] V. A. Kramarenko,[37] G. Kramberger,[92] P. Kramer,[99] M. W. Krasny,[126] A. Krasznahorkay,[36] J. A. Kremer,[99] T. Kresse,[50] J. Kretzschmar,[91] K. Kreul,[18] P. Krieger,[154] F. Krieter,[108] S. Krishnamurthy,[102] A. Krishnan,[63b] M. Krivos,[132] K. Krizka,[17a] K. Kroeninger,[49] H. Kroha,[109] J. Kroll,[130] J. Kroll,[127] K. S. Krowpman,[106] U. Kruchonak,[38] H. Krüger,[24] N. Krumnack,[80] M. C. Kruse,[51] J. A. Krzysiak,[85] A. Kubota,[153] O. Kuchinskaia,[37] S. Kuday,[3a] D. Kuechler,[48] J. T. Kuechler,[48] S. Kuehn,[36] T. Kuhl,[48] V. Kukhtin,[38] Y. Kulchitsky,[37,l] S. Kuleshov,[136d,136b] M. Kumar,[33g] N. Kumari,[101] M. Kuna,[60] A. Kupco,[130] T. Kupfer,[49] A. Kupich,[37] O. Kuprash,[54] H. Kurashige,[83] L. L. Kurchaninov,[155a] Y. A. Kurochkin,[37] A. Kurova,[37] E. S. Kuwertz,[36] M. Kuze,[153] A. K. Kvam,[102] J. Kvita,[121] T. Kwan,[103] K. W. Kwok,[64a] C. Lacasta,[161] F. Lacava,[74a,74b] H. Lacker,[18] D. Lacour,[126] N. N. Lad,[95] E. Ladygin,[38] B. Laforge,[126] T. Lagouri,[136e] S. Lai,[55] I. K. Lakomiec,[84a] N. Lalloue,[60] J. E. Lambert,[119] S. Lammers,[67] W. Lampl,[7] C. Lampoudis,[151] A. N. Lancaster,[114] E. Lançon,[29] U. Landgraf,[54] M. P. J. Landon,[93] V. S. Lang,[54] R. J. Langenberg,[102] A. J. Lankford,[158] F. Lanni,[29] K. Lantzsch,[24] A. Lanza,[72a] A. Lapertosa,[57b,57a] J. F. Laporte,[134] T. Lari,[70a] F. Lasagni Manghi,[23b] M. Lassnig,[36] V. Latonova,[130] T. S. Lau,[64a] A. Laudrain,[99] A. Laurier,[34] S. D. Lawlor,[94] Z. Lawrence,[100] M. Lazzaroni,[70a,70b] B. Le,[100] B. Leban,[92] A. Lebedev,[80] M. LeBlanc,[36] T. LeCompte,[6] F. Ledroit-Guillon,[60] A. C. A. Lee,[95] G. R. Lee,[16] L. Lee,[61] S. C. Lee,[147] S. Lee,[47a,47b] L. L. Leeuw,[33c] H. P. Lefebvre,[94] M. Lefebvre,[163] C. Leggett,[17a] K. Lehmann,[141] G. Lehmann Miotto,[36] W. A. Leight,[102] A. Leisos,[151,ab] M. A. L. Leite,[81c] C. E. Leitgeb,[48] R. Leitner,[132] K. J. C. Leney,[44] T. Lenz,[24] S. Leone,[73a] C. Leonidopoulos,[52] A. Leopold,[143] C. Leroy,[107] R. Les,[106] C. G. Lester,[32] M. Levchenko,[37] J. Levêque,[4] D. Levin,[105] L. J. Levinson,[167] D. J. Lewis,[20] B. Li,[14b] B. Li,[62b] C. Li,[62a] C-Q. Li,[62c,62d] H. Li,[62a] H. Li,[62b] H. Li,[14c] H. Li,[62b] J. Li,[62c] K. Li,[137] L. Li,[62c] M. Li,[14a,14d] Q. Y. Li,[62a] S. Li,[62d,62c,ac] T. Li,[62b] X. Li,[103] Z. Li,[62b] Z. Li,[125] Z. Li,[103] Z. Li,[91] Z. Liang,[14a] M. Liberatore,[48] B. Liberti,[75a] K. Lie,[64c] J. Lieber Marin,[81b] K. Lin,[106] R. A. Linck,[67] R. E. Lindley,[7] J. H. Lindon,[2] A. Linss,[48] E. Lipeles,[127] A. Lipniacka,[16] T. M. Liss,[160,ad] A. Lister,[162] J. D. Little,[4] B. Liu,[14a] B. X. Liu,[141] D. Liu,[62d,62c] J. B. Liu,[62a] J. K. K. Liu,[32] K. Liu,[62d,62c] M. Liu,[62a] M. Y. Liu,[62a] P. Liu,[14a] Q. Liu,[62d,137,62c] X. Liu,[62a] Y. Liu,[48] Y. Liu,[14c,14d] Y. L. Liu,[105] Y. W. Liu,[62a] M. Livan,[72a,72b] J. Llorente Merino,[141] S. L. Lloyd,[93] E. M. Lobodzinska,[48] P. Loch,[7] S. Loffredo,[75a,75b] T. Lohse,[18] K. Lohwasser,[138] M. Lokajicek,[130] J. D. Long,[160] I. Longarini,[74a,74b] L. Longo,[69a,69b] R. Longo,[160] I. Lopez Paz,[36] A. Lopez Solis,[48] J. Lorenz,[108] N. Lorenzo Martinez,[4] A. M. Lory,[108] A. Lösle,[54] X. Lou,[47a,47b] X. Lou,[14a,14d] A. Lounis,[66] J. Love,[6] P. A. Love,[90] J. J. Lozano Bahilo,[161] G. Lu,[14a,14d] M. Lu,[79] S. Lu,[127] Y. J. Lu,[65] H. J. Lubatti,[137] C. Luci,[74a,74b] F. L. Lucio Alves,[14c] A. Lucotte,[60] F. Luehring,[67] I. Luise,[144] O. Lukianchuk,[66] O. Lundberg,[143] B. Lund-Jensen,[143] N. A. Luongo,[122] M. S. Lutz,[150] D. Lynn,[29] H. Lyons,[91] R. Lysak,[130] E. Lytken,[97] F. Lyu,[14a] V. Lyubushkin,[38] T. Lyubushkina,[38] H. Ma,[29] L. L. Ma,[62b] Y. Ma,[95] D. M. Mac Donell,[163] G. Maccarrone,[53] J. C. MacDonald,[138] R. Madar,[40] W. F. Mader,[50] J. Maeda,[83] T. Maeno,[29] M. Maerker,[50] V. Magerl,[54] J. Magro,[68a,68c] H. Maguire,[138] D. J. Mahon,[41] C. Maidantchik,[81b] A. Maio,[129a,129b,129d] K. Maj,[84a] O. Majersky,[28a] S. Majewski,[122] N. Makovec,[66] V. Maksimovic,[15] B. Malaescu,[126] Pa. Malecki,[85] V. P. Maleev,[37] F. Malek,[60] D. Malito,[43b,43a] U. Mallik,[79] C. Malone,[32] S. Maltezos,[10] S. Malyukov,[38] J. Mamuzic,[13] G. Mancini,[53] G. Manco,[72a,72b] J. P. Mandalia,[93] I. Mandić,[92] L. Manhaes de Andrade Filho,[81a] I. M. Maniatis,[151] M. Manisha,[134] J. Manjarres Ramos,[50] D. C. Mankad,[167] K. H. Mankinen,[97] A. Mann,[108] A. Manousos,[78] B. Mansoulie,[134] S. Manzoni,[36] A. Marantis,[151] G. Marchiori,[5] M. Marcisovsky,[130] L. Marcoccia,[75a,75b] C. Marcon,[97] M. Marinescu,[20] M. Marjanovic,[119] Z. Marshall,[17a]

S. Marti-Garcia,[161] T. A. Martin,[165] V. J. Martin,[52] B. Martin dit Latour,[16] L. Martinelli,[74a,74b] M. Martinez,[13,w] P. Martinez Agullo,[161] V. I. Martinez Outschoorn,[102] P. Martinez Suarez,[13] S. Martin-Haugh,[133] V. S. Martoiu,[27b] A. C. Martyniuk,[95] A. Marzin,[36] S. R. Maschek,[109] L. Masetti,[99] T. Mashimo,[152] J. Masik,[100] A. L. Maslennikov,[37] L. Massa,[23b] P. Massarotti,[71a,71b] P. Mastrandrea,[73a,73b] A. Mastroberardino,[43b,43a] T. Masubuchi,[152] T. Mathisen,[159] A. Matic,[108] N. Matsuzawa,[152] J. Maurer,[27b] B. Maček,[92] D. A. Maximov,[37] R. Mazini,[147] I. Maznas,[151] M. Mazza,[106] S. M. Mazza,[135] C. Mc Ginn,[29,s] J. P. Mc Gowan,[103] S. P. Mc Kee,[105] T. G. McCarthy,[109] W. P. McCormack,[17a] E. F. McDonald,[104] A. E. McDougall,[113] J. A. Mcfayden,[145] G. Mchedlidze,[148b] R. P. Mckenzie,[33g] T. C. Mclachlan,[48] D. J. Mclaughlin,[95] K. D. McLean,[163] S. J. McMahon,[133] P. C. McNamara,[104] R. A. McPherson,[163,p] J. E. Mdhluli,[33g] S. Meehan,[36] T. Megy,[40] S. Mehlhase,[108] A. Mehta,[91] B. Meirose,[45] D. Melini,[149] B. R. Mellado Garcia,[33g] A. H. Melo,[55] F. Meloni,[48] E. D. Mendes Gouveia,[129a] A. M. Mendes Jacques Da Costa,[20] H. Y. Meng,[154] L. Meng,[90] S. Menke,[109] M. Mentink,[36] E. Meoni,[43b,43a] C. Merlassino,[125] L. Merola,[71a,71b] C. Meroni,[70a] G. Merz,[105] O. Meshkov,[37] J. K. R. Meshreki,[140] J. Metcalfe,[6] A. S. Mete,[6] C. Meyer,[67] J.-P. Meyer,[134] M. Michetti,[18] R. P. Middleton,[133] L. Mijović,[52] G. Mikenberg,[167] M. Mikestikova,[130] M. Mikuž,[92] H. Mildner,[138] A. Milic,[154] C. D. Milke,[44] D. W. Miller,[39] L. S. Miller,[34] A. Milov,[167] D. A. Milstead,[47a,47b] T. Min,[14c] A. A. Minaenko,[37] I. A. Minashvili,[148b] L. Mince,[59] A. I. Mincer,[116] B. Mindur,[84a] M. Mineev,[38] Y. Minegishi,[152] Y. Mino,[86] L. M. Mir,[13] M. Miralles Lopez,[161] M. Mironova,[125] T. Mitani,[166] A. Mitra,[165] V. A. Mitsou,[161] O. Miu,[154] P. S. Miyagawa,[93] Y. Miyazaki,[88] A. Mizukami,[82] J. U. Mjörnmark,[97] T. Mkrtchyan,[63a] M. Mlynarikova,[114] T. Moa,[47a,47b] S. Mobius,[55] K. Mochizuki,[107] P. Moder,[48] P. Mogg,[108] A. F. Mohammed,[14a,14d] S. Mohapatra,[41] G. Mokgatitswane,[33g] B. Mondal,[140] S. Mondal,[131] K. Mönig,[48] E. Monnier,[101] L. Monsonis Romero,[161] J. Montejo Berlingen,[36] M. Montella,[118] F. Monticelli,[89] N. Morange,[66] A. L. Moreira De Carvalho,[129a] M. Moreno Llácer,[161] C. Moreno Martinez,[13] P. Morettini,[57b] S. Morgenstern,[165] M. Morii,[61] M. Morinaga,[152] V. Morisbak,[124] A. K. Morley,[36] F. Morodei,[74a,74b] L. Morvaj,[36] P. Moschovakos,[36] B. Moser,[36] M. Mosidze,[148b] T. Moskalets,[54] P. Moskvitina,[112] J. Moss,[31,ae] E. J. W. Moyse,[102] S. Muanza,[101] J. Mueller,[128] D. Muenstermann,[90] R. Müller,[19] G. A. Mullier,[97] J. J. Mullin,[127] D. P. Mungo,[70a,70b] J. L. Munoz Martinez,[13] D. Munoz Perez,[161] F. J. Munoz Sanchez,[100] M. Murin,[100] W. J. Murray,[165,133] A. Murrone,[70a,70b] J. M. Muse,[119] M. Muškinja,[17a] C. Mwewa,[29] A. G. Myagkov,[37,l] A. J. Myers,[8] A. A. Myers,[128] G. Myers,[67] M. Myska,[131] B. P. Nachman,[17a] O. Nackenhorst,[49] A. Nag,[50] K. Nagai,[125] K. Nagano,[82] J. L. Nagle,[29,s] E. Nagy,[101] A. M. Nairz,[36] Y. Nakahama,[82] K. Nakamura,[82] H. Nanjo,[123] R. Narayan,[44] E. A. Narayanan,[111] I. Naryshkin,[37] M. Naseri,[34] C. Nass,[24] G. Navarro,[22a] J. Navarro-Gonzalez,[161] R. Nayak,[150] P. Y. Nechaeva,[37] F. Nechansky,[48] T. J. Neep,[20] A. Negri,[72a,72b] M. Negrini,[23b] C. Nellist,[112] C. Nelson,[103] K. Nelson,[105] S. Nemecek,[130] M. Nessi,[36,af] M. S. Neubauer,[160] F. Neuhaus,[99] J. Neundorf,[48] R. Newhouse,[162] P. R. Newman,[20] C. W. Ng,[128] Y. S. Ng,[18] Y. W. Y. Ng,[158] B. Ngair,[35e] H. D. N. Nguyen,[107] R. B. Nickerson,[125] R. Nicolaidou,[134] J. Nielsen,[135] M. Niemeyer,[55] N. Nikiforou,[36] V. Nikolaenko,[37,l] I. Nikolic-Audit,[126] K. Nikolopoulos,[20] P. Nilsson,[29] H. R. Nindhito,[56] A. Nisati,[74a] N. Nishu,[2] R. Nisius,[109] J.-E. Nitschke,[50] E. K. Nkadimeng,[33g] S. J. Noacco Rosende,[89] T. Nobe,[152] D. L. Noel,[32] Y. Noguchi,[86] T. Nommensen,[146] M. A. Nomura,[29] M. B. Norfolk,[138] R. R. B. Norisam,[95] B. J. Norman,[34] J. Novak,[92] T. Novak,[48] O. Novgorodova,[50] L. Novotny,[131] R. Novotny,[111] L. Nozka,[121] K. Ntekas,[158] E. Nurse,[95] F. G. Oakham,[34,d] J. Ocariz,[126] A. Ochi,[83] I. Ochoa,[129a] S. Oda,[88] S. Oerdek,[159] A. Ogrodnik,[84a] A. Oh,[100] C. C. Ohm,[143] H. Oide,[153] R. Oishi,[152] M. L. Ojeda,[48] Y. Okazaki,[86] M. W. O'Keefe,[91] Y. Okumura,[152] A. Olariu,[27b] L. F. Oleiro Seabra,[129a] S. A. Olivares Pino,[136e] D. Oliveira Damazio,[29] D. Oliveira Goncalves,[81a] J. L. Oliver,[158] M. J. R. Olsson,[158] A. Olszewski,[85] J. Olszowska,[85,i] Ö. O. Öncel,[54] D. C. O'Neil,[141] A. P. O'Neill,[19] A. Onofre,[129a,129e] P. U. E. Onyisi,[11] M. J. Oreglia,[39] G. E. Orellana,[89] D. Orestano,[76a,76b] N. Orlando,[13] R. S. Orr,[154] V. O'Shea,[59] R. Ospanov,[62a] G. Otero y Garzon,[30] H. Otono,[88] P. S. Ott,[63a] G. J. Ottino,[17a] M. Ouchrif,[35d] J. Ouellette,[29,s] F. Ould-Saada,[124] M. Owen,[59] R. E. Owen,[133] K. Y. Oyulmaz,[21a] V. E. Ozcan,[21a] N. Ozturk,[8] S. Ozturk,[21d] J. Pacalt,[121] H. A. Pacey,[32] K. Pachal,[51] A. Pacheco Pages,[13] C. Padilla Aranda,[13] G. Padovano,[74a,74b] S. Pagan Griso,[17a] G. Palacino,[67] A. Palazzo,[69a,69b] S. Palazzo,[52] S. Palestini,[36] M. Palka,[84b] J. Pan,[170] T. Pan,[64a] D. K. Panchal,[11] C. E. Pandini,[113] J. G. Panduro Vazquez,[94] P. Pani,[48] G. Panizzo,[68a,68c] L. Paolozzi,[56] C. Papadatos,[107] S. Parajuli,[44] A. Paramonov,[6] C. Paraskevopoulos,[10] D. Paredes Hernandez,[64b] T. H. Park,[154] M. A. Parker,[32] F. Parodi,[57b,57a] E. W. Parrish,[114] V. A. Parrish,[52] J. A. Parsons,[41] U. Parzefall,[54] B. Pascual Dias,[107] L. Pascual Dominguez,[150] V. R. Pascuzzi,[17a] F. Pasquali,[113] E. Pasqualucci,[74a] S. Passaggio,[57b] F. Pastore,[94] P. Pasuwan,[47a,47b] J. R. Pater,[100] J. Patton,[91] T. Pauly,[36] J. Pearkes,[142] M. Pedersen,[124] R. Pedro,[129a] S. V. Peleganchuk,[37] O. Penc,[130] C. Peng,[64b] H. Peng,[62a] M. Penzin,[37] B. S. Peralva,[81a,81d] A. P. Pereira Peixoto,[60] L. Pereira Sanchez,[47a,47b] D. V. Perepelitsa,[29,s] E. Perez Codina,[155a] M. Perganti,[10] L. Perini,[70a,70b,i] H. Pernegger,[36] S. Perrella,[36] A. Perrevoort,[112] O. Perrin,[40] K. Peters,[48] R. F. Y. Peters,[100] B. A. Petersen,[36] T. C. Petersen,[42] E. Petit,[101] V. Petousis,[131] C. Petridou,[151] A. Petrukhin,[140] M. Pettee,[17a] N. E. Pettersson,[36] A. Petukhov,[37] K. Petukhova,[132] A. Peyaud,[134] R. Pezoa,[136f] L. Pezzotti,[36] G. Pezzullo,[170] T. Pham,[104] P. W. Phillips,[133] M. W. Phipps,[160] G. Piacquadio,[144] E. Pianori,[17a] F. Piazza,[70a,70b] R. Piegaia,[30]

D. Pietreanu,[27b] A. D. Pilkington,[100] M. Pinamonti,[68a,68c] J. L. Pinfold,[2] B. C. Pinheiro Pereira,[129a] C. Pitman Donaldson,[95] D. A. Pizzi,[34] L. Pizzimento,[75a,75b] A. Pizzini,[113] M.-A. Pleier,[29] V. Plesanovs,[54] V. Pleskot,[132] E. Plotnikova,[38] G. Poddar,[4] R. Poettgen,[97] R. Poggi,[56] L. Poggioli,[126] I. Pogrebnyak,[106] D. Pohl,[24] I. Pokharel,[55] S. Polacek,[132] G. Polesello,[72a] A. Poley,[141,155a] R. Polifka,[131] A. Polini,[23b] C. S. Pollard,[125] Z. B. Pollock,[118] V. Polychronakos,[29] D. Ponomarenko,[37] L. Pontecorvo,[36] S. Popa,[27a] G. A. Popeneciu,[27d] D. M. Portillo Quintero,[155a] S. Pospisil,[131] P. Postolache,[27c] K. Potamianos,[125] I. N. Potrap,[38] C. J. Potter,[32] H. Potti,[1] T. Poulsen,[48] J. Poveda,[161] G. Pownall,[48] M. E. Pozo Astigarraga,[36] A. Prades Ibanez,[161] M. M. Prapa,[46] D. Price,[100] M. Primavera,[69a] M. A. Principe Martin,[98] M. L. Proffitt,[137] N. Proklova,[37] K. Prokofiev,[64c] G. Proto,[75a,75b] S. Protopopescu,[29] J. Proudfoot,[6] M. Przybycien,[84a] J. E. Puddefoot,[138] D. Pudzha,[37] P. Puzo,[66] D. Pyatiizbyantseva,[37] J. Qian,[105] Y. Qin,[100] T. Qiu,[93] A. Quadt,[55] M. Queitsch-Maitland,[24] G. Rabanal Bolanos,[61] D. Rafanoharana,[54] F. Ragusa,[70a,70b] J. L. Rainbolt,[39] J. A. Raine,[56] S. Rajagopalan,[29] E. Ramakoti,[37] K. Ran,[14a,14d] V. Raskina,[126] D. F. Rassloff,[63a] S. Rave,[99] B. Ravina,[59] I. Ravinovich,[167] M. Raymond,[36] A. L. Read,[124] N. P. Readioff,[138] D. M. Rebuzzi,[72a,72b] G. Redlinger,[29] K. Reeves,[45] J. A. Reidelsturz,[169] D. Reikher,[150] A. Reiss,[99] A. Rej,[140] C. Rembser,[36] A. Renardi,[48] M. Renda,[27b] M. B. Rendel,[109] A. G. Rennie,[59] S. Resconi,[70a] M. Ressegotti,[57b,57a] E. D. Resseguie,[17a] S. Rettie,[95] B. Reynolds,[118] E. Reynolds,[17a] M. Rezaei Estabragh,[169] O. L. Rezanova,[37] P. Reznicek,[132] E. Ricci,[77a,77b] R. Richter,[109] S. Richter,[47a,47b] E. Richter-Was,[84b] M. Ridel,[126] P. Rieck,[116] P. Riedler,[36] M. Rijssenbeek,[144] A. Rimoldi,[72a,72b] M. Rimoldi,[48] L. Rinaldi,[23b,23a] T. T. Rinn,[29] M. P. Rinnagel,[108] G. Ripellino,[143] I. Riu,[13] P. Rivadeneira,[48] J. C. Rivera Vergara,[163] F. Rizatdinova,[120] E. Rizvi,[93] C. Rizzi,[56] B. A. Roberts,[165] B. R. Roberts,[17a] S. H. Robertson,[103,p] M. Robin,[48] D. Robinson,[32] C. M. Robles Gajardo,[136f] M. Robles Manzano,[99] A. Robson,[59] A. Rocchi,[75a,75b] C. Roda,[73a,73b] S. Rodriguez Bosca,[63a] Y. Rodriguez Garcia,[22a] A. Rodriguez Rodriguez,[54] A. M. Rodríguez Vera,[155b] S. Roe,[36] J. T. Roemer,[158] A. R. Roepe-Gier,[119] J. Roggel,[169] O. Røhne,[124] R. A. Rojas,[163] B. Roland,[54] C. P. A. Roland,[67] J. Roloff,[29] A. Romaniouk,[37] E. Romano,[72a,72b] M. Romano,[23b] A. C. Romero Hernandez,[160] N. Rompotis,[91] L. Roos,[126] S. Rosati,[74a] B. J. Rosser,[39] E. Rossi,[4] E. Rossi,[71a,71b] L. P. Rossi,[57b] L. Rossini,[48] R. Rosten,[118] M. Rotaru,[27b] B. Rottler,[54] D. Rousseau,[66] D. Rousso,[32] G. Rovelli,[72a,72b] A. Roy,[160] A. Rozanov,[101] Y. Rozen,[149] X. Ruan,[33g] A. Rubio Jimenez,[161] A. J. Ruby,[91] T. A. Ruggeri,[1] F. Rühr,[54] A. Ruiz-Martinez,[161] A. Rummler,[36] Z. Rurikova,[54] N. A. Rusakovich,[38] H. L. Russell,[163] J. P. Rutherfoord,[7] E. M. Rüttinger,[138] K. Rybacki,[90] M. Rybar,[132] E. B. Rye,[124] A. Ryzhov,[37] J. A. Sabater Iglesias,[56] P. Sabatini,[161] L. Sabetta,[74a,74b] H.F-W. Sadrozinski,[135] F. Safai Tehrani,[74a] B. Safarzadeh Samani,[145] M. Safdari,[142] S. Saha,[103] M. Sahinsoy,[109] M. Saimpert,[134] M. Saito,[152] T. Saito,[152] D. Salamani,[36] G. Salamanna,[76a,76b] A. Salnikov,[142] J. Salt,[161] A. Salvador Salas,[13] D. Salvatore,[43b,43a] F. Salvatore,[145] A. Salzburger,[36] D. Sammel,[54] D. Sampsonidis,[151] D. Sampsonidou,[62d,62c] J. Sánchez,[161] A. Sanchez Pineda,[4] V. Sanchez Sebastian,[161] H. Sandaker,[124] C. O. Sander,[48] J. A. Sandesara,[102] M. Sandhoff,[169] C. Sandoval,[22b] D. P. C. Sankey,[133] A. Sansoni,[53] L. Santi,[74a,74b] C. Santoni,[40] H. Santos,[129a,129b] S. N. Santpur,[17a] A. Santra,[167] K. A. Saoucha,[138] J. G. Saraiva,[129a,129d] J. Sardain,[101] O. Sasaki,[82] K. Sato,[156] C. Sauer,[63b] F. Sauerburger,[54] E. Sauvan,[4] P. Savard,[154,d] R. Sawada,[152] C. Sawyer,[133] L. Sawyer,[96] I. Sayago Galvan,[161] C. Sbarra,[23b] A. Sbrizzi,[23b,23a] T. Scanlon,[95] J. Schaarschmidt,[137] P. Schacht,[109] D. Schaefer,[39] U. Schäfer,[99] A. C. Schaffer,[66] D. Schaile,[108] R. D. Schamberger,[144] E. Schanet,[108] C. Scharf,[18] V. A. Schegelsky,[37] D. Scheirich,[132] F. Schenck,[18] M. Schernau,[158] C. Scheulen,[55] C. Schiavi,[57b,57a] Z. M. Schillaci,[26] E. J. Schioppa,[69a,69b] M. Schioppa,[43b,43a] B. Schlag,[99] K. E. Schleicher,[54] S. Schlenker,[36] K. Schmieden,[99] C. Schmitt,[99] S. Schmitt,[48] L. Schoeffel,[134] A. Schoening,[63b] P. G. Scholer,[54] E. Schopf,[125] M. Schott,[99] J. Schovancova,[36] S. Schramm,[56] F. Schroeder,[169] H-C. Schultz-Coulon,[63a] M. Schumacher,[54] B. A. Schumm,[135] Ph. Schune,[134] A. Schwartzman,[142] T. A. Schwarz,[105] Ph. Schwemling,[134] R. Schwienhorst,[106] A. Sciandra,[135] G. Sciolla,[26] F. Scuri,[73a] F. Scutti,[104] C. D. Sebastiani,[91] K. Sedlaczek,[49] P. Seema,[18] S. C. Seidel,[111] A. Seiden,[135] B. D. Seidlitz,[41] T. Seiss,[39] C. Seitz,[48] J. M. Seixas,[81b] G. Sekhniaidze,[71a] S. J. Sekula,[44] L. Selem,[4] N. Semprini-Cesari,[23b,23a] S. Sen,[51] D. Sengupta,[56] V. Senthilkumar,[161] L. Serin,[66] L. Serkin,[68a,68b] M. Sessa,[76a,76b] H. Severini,[119] S. Sevova,[142] F. Sforza,[57b,57a] A. Sfyrla,[56] E. Shabalina,[55] R. Shaheen,[143] J. D. Shahinian,[127] N. W. Shaikh,[47a,47b] D. Shaked Renous,[167] L. Y. Shan,[14a] M. Shapiro,[17a] A. Sharma,[36] A. S. Sharma,[162] P. Sharma,[79] S. Sharma,[48] P. B. Shatalov,[37] K. Shaw,[145] S. M. Shaw,[100] Q. Shen,[62c] P. Sherwood,[95] L. Shi,[95] C. O. Shimmin,[170] Y. Shimogama,[166] J. D. Shinner,[94] I. P. J. Shipsey,[125] S. Shirabe,[60] M. Shiyakova,[38] J. Shlomi,[167] M. J. Shochet,[39] J. Shojaii,[104] D. R. Shope,[143] S. Shrestha,[118] E. M. Shrif,[33g] M. J. Shroff,[163] P. Sicho,[130] A. M. Sickles,[160] E. Sideras Haddad,[33g] O. Sidiropoulou,[36] A. Sidoti,[23b] F. Siegert,[50] Dj. Sijacki,[15] R. Sikora,[84a] F. Sili,[89] J. M. Silva,[20] M. V. Silva Oliveira,[36] S. B. Silverstein,[47a] S. Simion,[66] R. Simoniello,[36] E. L. Simpson,[59] N. D. Simpson,[97] S. Simsek,[21d] S. Sindhu,[55] P. Sinervo,[154] V. Sinetckii,[37] S. Singh,[141] S. Singh,[154] S. Sinha,[48] S. Sinha,[33g] M. Sioli,[23b,23a] I. Siral,[122] S.Yu. Sivoklokov,[37,i] J. Sjölin,[47a,47b] A. Skaf,[55] E. Skorda,[97] P. Skubic,[119] M. Slawinska,[85] V. Smakhtin,[167] B. H. Smart,[133] J. Smiesko,[132] S.Yu. Smirnov,[37] Y. Smirnov,[37] L. N. Smirnova,[37,1] O. Smirnova,[97] E. A. Smith,[39] H. A. Smith,[125] J. L. Smith,[91] R. Smith,[142] M. Smizanska,[90]

K. Smolek,[131] A. Smykiewicz,[85] A. A. Snesarev,[37] H. L. Snoek,[113] S. Snyder,[29] R. Sobie,[163,p] A. Soffer,[150] C. A. Solans Sanchez,[36] E.Yu. Soldatov,[37] U. Soldevila,[161] A. A. Solodkov,[37] S. Solomon,[54] A. Soloshenko,[38] K. Solovieva,[54] O. V. Solovyanov,[37] V. Solovyev,[37] P. Sommer,[36] A. Sonay,[13] W. Y. Song,[155b] A. Sopczak,[131] A. L. Sopio,[95] F. Sopkova,[28b] V. Sothilingam,[63a] S. Sottocornola,[72a,72b] R. Soualah,[115c] Z. Soumaimi,[35e] D. South,[48] S. Spagnolo,[69a,69b] M. Spalla,[109] F. Spanò,[94] D. Sperlich,[54] G. Spigo,[36] M. Spina,[145] S. Spinali,[90] D. P. Spiteri,[59] M. Spousta,[132] E. J. Staats,[34] A. Stabile,[70a,70b] R. Stamen,[63a] M. Stamenkovic,[113] A. Stampekis,[20] M. Standke,[24] E. Stanecka,[85] B. Stanislaus,[17a] M. M. Stanitzki,[48] M. Stankaityte,[125] B. Stapf,[48] E. A. Starchenko,[37] G. H. Stark,[135] J. Stark,[101] D. M. Starko,[155b] P. Staroba,[130] P. Starovoitov,[63a] S. Stärz,[103] R. Staszewski,[85] G. Stavropoulos,[46] J. Steentoft,[159] P. Steinberg,[29] A. L. Steinhebel,[122] B. Stelzer,[141,155a] H. J. Stelzer,[128] O. Stelzer-Chilton,[155a] H. Stenzel,[58] T. J. Stevenson,[145] G. A. Stewart,[36] M. C. Stockton,[36] G. Stoicea,[27b] M. Stolarski,[129a] S. Stonjek,[109] A. Straessner,[50] J. Strandberg,[143] S. Strandberg,[47a,47b] M. Strauss,[119] T. Strebler,[101] P. Strizenec,[28b] R. Ströhmer,[164] D. M. Strom,[122] L. R. Strom,[48] R. Stroynowski,[44] A. Strubig,[47a,47b] S. A. Stucci,[29] B. Stugu,[16] J. Stupak,[119] N. A. Styles,[48] D. Su,[142] S. Su,[62a] W. Su,[62d,137,62c] X. Su,[62a,66] K. Sugizaki,[152] V. V. Sulin,[37] M. J. Sullivan,[91] D. M. S. Sultan,[77a,77b] L. Sultanaliyeva,[37] S. Sultansoy,[3b] T. Sumida,[86] S. Sun,[105] S. Sun,[168] O. Sunneborn Gudnadottir,[159] M. R. Sutton,[145] M. Svatos,[130] M. Swiatlowski,[155a] T. Swirski,[164] I. Sykora,[28a] M. Sykora,[132] T. Sykora,[132] D. Ta,[99] K. Tackmann,[48,ag] A. Taffard,[158] R. Tafirout,[155a] J. S. Tafoya Vargas,[66] R. H. M. Taibah,[126] R. Takashima,[87] K. Takeda,[83] E. P. Takeva,[52] Y. Takubo,[82] M. Talby,[101] A. A. Talyshev,[37] K. C. Tam,[64b] N. M. Tamir,[150] A. Tanaka,[152] J. Tanaka,[152] R. Tanaka,[66] M. Tanasini,[57b,57a] J. Tang,[62c] Z. Tao,[162] S. Tapia Araya,[80] S. Tapprogge,[99] A. Tarek Abouelfadl Mohamed,[106] S. Tarem,[149] K. Tariq,[62b] G. Tarna,[27b] G. F. Tartarelli,[70a] P. Tas,[132] M. Tasevsky,[130] E. Tassi,[43b,43a] A. C. Tate,[160] G. Tateno,[152] Y. Tayalati,[35e] G. N. Taylor,[104] W. Taylor,[155b] H. Teagle,[91] A. S. Tee,[168] R. Teixeira De Lima,[142] P. Teixeira-Dias,[94] J. J. Teoh,[154] K. Terashi,[152] J. Terron,[98] S. Terzo,[13] M. Testa,[53] R. J. Teuscher,[154,p] N. Themistokleous,[52] T. Theveneaux-Pelzer,[18] O. Thielmann,[169] D. W. Thomas,[94] J. P. Thomas,[20] E. A. Thompson,[48] P. D. Thompson,[20] E. Thomson,[127] E. J. Thorpe,[93] Y. Tian,[55] V. Tikhomirov,[37,1] Yu. A. Tikhonov,[37] S. Timoshenko,[37] E. X. L. Ting,[1] P. Tipton,[170] S. Tisserant,[101] S. H. Tlou,[33g] A. Tnourji,[40] K. Todome,[23b,23a] S. Todorova-Nova,[132] S. Todt,[50] M. Togawa,[82] J. Tojo,[88] S. Tokár,[28a] K. Tokushuku,[82] R. Tombs,[32] M. Tomoto,[82,110] L. Tompkins,[142] P. Tornambe,[102] E. Torrence,[122] H. Torres,[50] E. Torró Pastor,[161] M. Toscani,[30] C. Tosciri,[39] D. R. Tovey,[138] A. Traeet,[16] I. S. Trandafir,[27b] T. Trefzger,[164] A. Tricoli,[29] I. M. Trigger,[155a] S. Trincaz-Duvoid,[126] D. A. Trischuk,[162] B. Trocmé,[60] A. Trofymov,[66] C. Troncon,[70a] L. Truong,[33c] M. Trzebinski,[85] A. Trzupek,[85] F. Tsai,[144] M. Tsai,[105] A. Tsiamis,[151] P. V. Tsiareshka,[37] S. Tsigaridas,[155a] A. Tsirigotis,[151,ab] V. Tsiskaridze,[144] E. G. Tskhadadze,[148a] M. Tsopoulou,[151] Y. Tsujikawa,[86] I. I. Tsukerman,[37] V. Tsulaia,[17a] S. Tsuno,[82] O. Tsur,[149] D. Tsybychev,[144] Y. Tu,[64b] A. Tudorache,[27b] V. Tudorache,[27b] A. N. Tuna,[36] S. Turchikhin,[38] I. Turk Cakir,[3a] R. Turra,[70a] P. M. Tuts,[41] S. Tzamarias,[151] P. Tzanis,[10] E. Tzovara,[99] K. Uchida,[152] F. Ukegawa,[156] P. A. Ulloa Poblete,[136c] G. Unal,[36] M. Unal,[11] A. Undrus,[29] G. Unel,[158] K. Uno,[152] J. Urban,[28b] P. Urquijo,[104] G. Usai,[8] R. Ushioda,[153] M. Usman,[107] Z. Uysal,[21b] V. Vacek,[131] B. Vachon,[103] K. O. H. Vadla,[124] T. Vafeiadis,[36] C. Valderanis,[108] E. Valdes Santurio,[47a,47b] M. Valente,[155a] S. Valentinetti,[23b,23a] A. Valero,[161] A. Vallier,[101] J. A. Valls Ferrer,[161] T. R. Van Daalen,[137] P. Van Gemmeren,[6] S. Van Stroud,[95] I. Van Vulpen,[113] M. Vanadia,[75a,75b] W. Vandelli,[36] M. Vandenbroucke,[134] E. R. Vandewall,[120] D. Vannicola,[150] L. Vannoli,[57b,57a] R. Vari,[74a] E. W. Varnes,[7] C. Varni,[17a] T. Varol,[147] D. Varouchas,[66] L. Varriale,[161] K. E. Varvell,[146] M. E. Vasile,[27b] L. Vaslin,[40] G. A. Vasquez,[163] F. Vazeille,[40] T. Vazquez Schroeder,[36] J. Veatch,[31] V. Vecchio,[100] M. J. Veen,[113] I. Veliscek,[125] L. M. Veloce,[154] F. Veloso,[129a,129c] S. Veneziano,[74a] A. Ventura,[69a,69b] A. Verbytskyi,[109] M. Verducci,[73a,73b] C. Vergis,[24] M. Verissimo De Araujo,[81b] W. Verkerke,[113] J. C. Vermeulen,[113] C. Vernieri,[142] P. J. Verschuuren,[94] M. Vessella,[102] M. L. Vesterbacka,[116] M. C. Vetterli,[141,d] A. Vgenopoulos,[151] N. Viaux Maira,[136f] T. Vickey,[138] O. E. Vickey Boeriu,[138] G. H. A. Viehhauser,[125] L. Vigani,[63b] M. Villa,[23b,23a] M. Villaplana Perez,[161] E. M. Villhauer,[52] E. Vilucchi,[53] M. G. Vincter,[34] G. S. Virdee,[20] A. Vishwakarma,[52] C. Vittori,[23b,23a] I. Vivarelli,[145] V. Vladimirov,[165] E. Voevodina,[109] F. Vogel,[108] P. Vokac,[131] J. Von Ahnen,[48] E. Von Toerne,[24] B. Vormwald,[36] V. Vorobel,[132] K. Vorobev,[37] M. Vos,[161] J. H. Vossebeld,[91] M. Vozak,[113] L. Vozdecky,[93] N. Vranjes,[15] M. Vranjes Milosavljevic,[15] M. Vreeswijk,[113] R. Vuillermet,[36] O. Vujinovic,[99] I. Vukotic,[39] S. Wada,[156] C. Wagner,[102] W. Wagner,[169] S. Wahdan,[169] H. Wahlberg,[89] R. Wakasa,[156] M. Wakida,[110] V. M. Walbrecht,[109] J. Walder,[133] R. Walker,[108] W. Walkowiak,[140] A. M. Wang,[61] A. Z. Wang,[168] C. Wang,[62a] C. Wang,[62c] H. Wang,[17a] J. Wang,[64a] P. Wang,[44] R.-J. Wang,[99] R. Wang,[61] R. Wang,[6] S. M. Wang,[147] S. Wang,[62b] T. Wang,[62a] W. T. Wang,[79] W. X. Wang,[62a] X. Wang,[14c] X. Wang,[160] X. Wang,[62c] Y. Wang,[62d] Y. Wang,[14c] Z. Wang,[105] Z. Wang,[62d,51,62c] Z. Wang,[105] A. Warburton,[103] R. J. Ward,[20] N. Warrack,[59] A. T. Watson,[20] M. F. Watson,[20] G. Watts,[137] B. M. Waugh,[95] A. F. Webb,[11] C. Weber,[29] M. S. Weber,[19] S. A. Weber,[34] S. M. Weber,[63a] C. Wei,[62a] Y. Wei,[125] A. R. Weidberg,[125] J. Weingarten,[49] M. Weirich,[99] C. Weiser,[54] C. J. Wells,[48] T. Wenaus,[29] B. Wendland,[49] T. Wengler,[36] N. S. Wenke,[109] N. Wermes,[24] M. Wessels,[63a] K. Whalen,[122] A. M. Wharton,[90] A. S. White,[61] A. White,[8] M. J. White,[1] D. Whiteson,[158]

L. Wickremasinghe,[123] W. Wiedenmann,[168] C. Wiel,[50] M. Wielers,[133] N. Wieseotte,[99] C. Wiglesworth,[42] L. A. M. Wiik-Fuchs,[54] D. J. Wilbern,[119] H. G. Wilkens,[36] D. M. Williams,[41] H. H. Williams,[127] S. Williams,[32] S. Willocq,[102] P. J. Windischhofer,[125] F. Winklmeier,[122] B. T. Winter,[54] M. Wittgen,[142] M. Wobisch,[96] A. Wolf,[99] R. Wölker,[125] J. Wollrath,[158] M. W. Wolter,[85] H. Wolters,[129a,129c] V. W. S. Wong,[162] A. F. Wongel,[48] S. D. Worm,[48] B. K. Wosiek,[85] K. W. Woźniak,[85] K. Wraight,[59] J. Wu,[14a,14d] M. Wu,[64a] S. L. Wu,[168] X. Wu,[56] Y. Wu,[62a] Z. Wu,[134,62a] J. Wuerzinger,[125] T. R. Wyatt,[100] B. M. Wynne,[52] S. Xella,[42] L. Xia,[14c] M. Xia,[14b] J. Xiang,[64c] X. Xiao,[105] M. Xie,[62a] X. Xie,[62a] J. Xiong,[17a] I. Xiotidis,[145] D. Xu,[14a] H. Xu,[62a] H. Xu,[62a] L. Xu,[62a] R. Xu,[127] T. Xu,[105] W. Xu,[105] Y. Xu,[14b] Z. Xu,[62b] Z. Xu,[142] B. Yabsley,[146] S. Yacoob,[33a] N. Yamaguchi,[88] Y. Yamaguchi,[153] H. Yamauchi,[156] T. Yamazaki,[17a] Y. Yamazaki,[83] J. Yan,[62c] S. Yan,[125] Z. Yan,[25] H. J. Yang,[62c,62d] H. T. Yang,[17a] S. Yang,[62a] T. Yang,[64c] X. Yang,[62a] X. Yang,[14a] Y. Yang,[44] Z. Yang,[62a,105] W-M. Yao,[17a] Y. C. Yap,[48] H. Ye,[14c] J. Ye,[44] S. Ye,[29] X. Ye,[62a] I. Yeletskikh,[38] M. R. Yexley,[90] P. Yin,[41] K. Yorita,[166] C. J. S. Young,[54] C. Young,[142] M. Yuan,[105] R. Yuan,[62b,ah] L. Yue,[95] X. Yue,[63a] M. Zaazoua,[35e] B. Zabinski,[85] E. Zaid,[52] T. Zakareishvili,[148b] N. Zakharchuk,[34] S. Zambito,[56] J. Zang,[152] D. Zanzi,[54] O. Zaplatilek,[131] S. V. Zeißner,[49] C. Zeitnitz,[169] J. C. Zeng,[160] D. T. Zenger Jr.,[26] O. Zenin,[37] T. Ženiš,[28a] S. Zenz,[93] S. Zerradi,[35a] D. Zerwas,[66] B. Zhang,[14c] D. F. Zhang,[138] G. Zhang,[14b] J. Zhang,[6] K. Zhang,[14a,14d] L. Zhang,[14c] R. Zhang,[168] S. Zhang,[105] T. Zhang,[152] X. Zhang,[62c] X. Zhang,[62b] Z. Zhang,[17a] Z. Zhang,[66] H. Zhao,[137] P. Zhao,[51] T. Zhao,[62b] Y. Zhao,[135] Z. Zhao,[62a] A. Zhemchugov,[38] Z. Zheng,[142] D. Zhong,[160] B. Zhou,[105] C. Zhou,[168] H. Zhou,[7] N. Zhou,[62c] Y. Zhou,[7] C. G. Zhu,[62b] C. Zhu,[14a,14d] H. L. Zhu,[62a] H. Zhu,[14a] J. Zhu,[105] Y. Zhu,[62a] X. Zhuang,[14a] K. Zhukov,[37] V. Zhulanov,[37] N. I. Zimine,[38] J. Zinsser,[63b] M. Ziolkowski,[140] L. Živković,[15] A. Zoccoli,[23b,23a] K. Zoch,[56] T. G. Zorbas,[138] O. Zormpa,[46] W. Zou,[41] and L. Zwalinski[36]

(ATLAS Collaboration)

[1]*Department of Physics, University of Adelaide, Adelaide, Australia*
[2]*Department of Physics, University of Alberta, Edmonton, Alberta, Canada*
[3a]*Department of Physics, Ankara University, Ankara, Türkiye*
[3b]*Division of Physics, TOBB University of Economics and Technology, Ankara, Türkiye*
[4]*LAPP, Université Savoie Mont Blanc, CNRS/IN2P3, Annecy, France*
[5]*APC, Université Paris Cité, CNRS/IN2P3, Paris, France*
[6]*High Energy Physics Division, Argonne National Laboratory, Argonne, Illinois, USA*
[7]*Department of Physics, University of Arizona, Tucson, Arizona, USA*
[8]*Department of Physics, University of Texas at Arlington, Arlington, Texas, USA*
[9]*Physics Department, National and Kapodistrian University of Athens, Athens, Greece*
[10]*Physics Department, National Technical University of Athens, Zografou, Greece*
[11]*Department of Physics, University of Texas at Austin, Austin, Texas, USA*
[12]*Institute of Physics, Azerbaijan Academy of Sciences, Baku, Azerbaijan*
[13]*Institut de Física d'Altes Energies (IFAE), Barcelona Institute of Science and Technology, Barcelona, Spain*
[14a]*Institute of High Energy Physics, Chinese Academy of Sciences, Beijing, China*
[14b]*Physics Department, Tsinghua University, Beijing, China*
[14c]*Department of Physics, Nanjing University, Nanjing, China*
[14d]*University of Chinese Academy of Science (UCAS), Beijing, China*
[15]*Institute of Physics, University of Belgrade, Belgrade, Serbia*
[16]*Department for Physics and Technology, University of Bergen, Bergen, Norway*
[17a]*Physics Division, Lawrence Berkeley National Laboratory, Berkeley, California, USA*
[17b]*University of California, Berkeley, California, USA*
[18]*Institut für Physik, Humboldt Universität zu Berlin, Berlin, Germany*
[19]*Albert Einstein Center for Fundamental Physics and Laboratory for High Energy Physics, University of Bern, Bern, Switzerland*
[20]*School of Physics and Astronomy, University of Birmingham, Birmingham, United Kingdom*
[21a]*Department of Physics, Bogazici University, Istanbul, Türkiye*
[21b]*Department of Physics Engineering, Gaziantep University, Gaziantep, Türkiye*
[21c]*Department of Physics, Istanbul University, Istanbul, Türkiye*
[21d]*Istinye University, Sariyer, Istanbul, Türkiye*
[22a]*Facultad de Ciencias y Centro de Investigaciónes, Universidad Antonio Nariño, Bogotá, Colombia*
[22b]*Departamento de Física, Universidad Nacional de Colombia, Bogotá, Colombia*
[23a]*Dipartimento di Fisica e Astronomia A. Righi, Università di Bologna, Bologna, Italy*
[23b]*INFN Sezione di Bologna, Italy*
[24]*Physikalisches Institut, Universität Bonn, Bonn, Germany*

[25]*Department of Physics, Boston University, Boston, Massachusetts, USA*
[26]*Department of Physics, Brandeis University, Waltham, Massachusetts, USA*
[27a]*Transilvania University of Brasov, Brasov, Romania*
[27b]*Horia Hulubei National Institute of Physics and Nuclear Engineering, Bucharest, Romania*
[27c]*Department of Physics, Alexandru Ioan Cuza University of Iasi, Iasi, Romania*
[27d]*Physics Department, National Institute for Research and Development of Isotopic and Molecular Technologies, Cluj-Napoca, Romania*
[27e]*University Politehnica Bucharest, Bucharest, Romania*
[27f]*West University in Timisoara, Timisoara, Romania*
[28a]*Faculty of Mathematics, Physics and Informatics, Comenius University, Bratislava, Slovak Republic*
[28b]*Department of Subnuclear Physics, Institute of Experimental Physics of the Slovak Academy of Sciences, Kosice, Slovak Republic*
[29]*Physics Department, Brookhaven National Laboratory, Upton, New York, USA*
[30]*Facultad de Ciencias Exactas y Naturales, Departamento de Física, Universidad de Buenos Aires, y CONICET, Instituto de Física de Buenos Aires (IFIBA), Buenos Aires, Argentina*
[31]*California State University, California, USA*
[32]*Cavendish Laboratory, University of Cambridge, Cambridge, United Kingdom*
[33a]*Department of Physics, University of Cape Town, Cape Town, South Africa*
[33b]*iThemba Labs, Western Cape, South Africa*
[33c]*Department of Mechanical Engineering Science, University of Johannesburg, Johannesburg, South Africa*
[33d]*National Institute of Physics, University of the Philippines Diliman (Philippines), South Africa*
[33e]*University of South Africa, Department of Physics, Pretoria, South Africa*
[33f]*University of Zululand, KwaDlangezwa, South Africa*
[33g]*School of Physics, University of the Witwatersrand, Johannesburg, South Africa*
[34]*Department of Physics, Carleton University, Ottawa, Ontario, Canada*
[35a]*Faculté des Sciences Ain Chock, Réseau Universitaire de Physique des Hautes Energies - Université Hassan II, Casablanca, Morocco*
[35b]*Faculté des Sciences, Université Ibn-Tofail, Kénitra, Morocco*
[35c]*Faculté des Sciences Semlalia, Université Cadi Ayyad, LPHEA-Marrakech, Morocco*
[35d]*LPMR, Faculté des Sciences, Université Mohamed Premier, Oujda, Morocco*
[35e]*Faculté des sciences, Université Mohammed V, Rabat, Morocco*
[35f]*Institute of Applied Physics, Mohammed VI Polytechnic University, Ben Guerir, Morocco*
[36]*CERN, Geneva, Switzerland*
[37]*Affiliated with an institute covered by a cooperation agreement with CERN*
[38]*Affiliated with an international laboratory covered by a cooperation agreement with CERN*
[39]*Enrico Fermi Institute, University of Chicago, Chicago, Illinois, USA*
[40]*LPC, Université Clermont Auvergne, CNRS/IN2P3, Clermont-Ferrand, France*
[41]*Nevis Laboratory, Columbia University, Irvington, New York, USA*
[42]*Niels Bohr Institute, University of Copenhagen, Copenhagen, Denmark*
[43a]*Dipartimento di Fisica, Università della Calabria, Rende, Italy*
[43b]*INFN Gruppo Collegato di Cosenza, Laboratori Nazionali di Frascati, Italy*
[44]*Physics Department, Southern Methodist University, Dallas, Texas, USA*
[45]*Physics Department, University of Texas at Dallas, Richardson, Texas, USA*
[46]*National Centre for Scientific Research "Demokritos", Agia Paraskevi, Greece*
[47a]*Department of Physics, Stockholm University, Sweden*
[47b]*Oskar Klein Centre, Stockholm, Sweden*
[48]*Deutsches Elektronen-Synchrotron DESY, Hamburg and Zeuthen, Germany*
[49]*Fakultät Physik, Technische Universität Dortmund, Dortmund, Germany*
[50]*Institut für Kern- und Teilchenphysik, Technische Universität Dresden, Dresden, Germany*
[51]*Department of Physics, Duke University, Durham, North Carolina, USA*
[52]*SUPA - School of Physics and Astronomy, University of Edinburgh, Edinburgh, United Kingdom*
[53]*INFN e Laboratori Nazionali di Frascati, Frascati, Italy*
[54]*Physikalisches Institut, Albert-Ludwigs-Universität Freiburg, Freiburg, Germany*
[55]*II. Physikalisches Institut, Georg-August-Universität Göttingen, Göttingen, Germany*
[56]*Département de Physique Nucléaire et Corpusculaire, Université de Genève, Genève, Switzerland*
[57a]*Dipartimento di Fisica, Università di Genova, Genova, Italy*
[57b]*INFN Sezione di Genova, Genova, Italy*
[58]*II. Physikalisches Institut, Justus-Liebig-Universität Giessen, Giessen, Germany*
[59]*SUPA - School of Physics and Astronomy, University of Glasgow, Glasgow, United Kingdom*
[60]*LPSC, Université Grenoble Alpes, CNRS/IN2P3, Grenoble INP, Grenoble, France*
[61]*Laboratory for Particle Physics and Cosmology, Harvard University, Cambridge, Massachusetts, USA*

[62a]*Department of Modern Physics and State Key Laboratory of Particle Detection and Electronics, University of Science and Technology of China, Hefei, China*
[62b]*Institute of Frontier and Interdisciplinary Science and Key Laboratory of Particle Physics and Particle Irradiation (MOE), Shandong University, Qingdao, China*
[62c]*School of Physics and Astronomy, Shanghai Jiao Tong University, Key Laboratory for Particle Astrophysics and Cosmology (MOE), SKLPPC, Shanghai, China*
[62d]*Tsung-Dao Lee Institute, Shanghai, China*
[63a]*Kirchhoff-Institut für Physik, Ruprecht-Karls-Universität Heidelberg, Heidelberg, Germany*
[63b]*Physikalisches Institut, Ruprecht-Karls-Universität Heidelberg, Heidelberg, Germany*
[64a]*Department of Physics, Chinese University of Hong Kong, Shatin, N.T., Hong Kong, China*
[64b]*Department of Physics, University of Hong Kong, Hong Kong, China*
[64c]*Department of Physics and Institute for Advanced Study, Hong Kong University of Science and Technology, Clear Water Bay, Kowloon, Hong Kong, China*
[65]*Department of Physics, National Tsing Hua University, Hsinchu, Taiwan*
[66]*IJCLab, Université Paris-Saclay, CNRS/IN2P3, 91405 Orsay, France*
[67]*Department of Physics, Indiana University, Bloomington, Indiana, USA*
[68a]*INFN Gruppo Collegato di Udine, Sezione di Trieste, Udine, Italy*
[68b]*ICTP, Trieste, Italy*
[68c]*Dipartimento Politecnico di Ingegneria e Architettura, Università di Udine, Udine, Italy*
[69a]*INFN Sezione di Lecce, Italy*
[69b]*Dipartimento di Matematica e Fisica, Università del Salento, Lecce, Italy*
[70a]*INFN Sezione di Milano, Italy*
[70b]*Dipartimento di Fisica, Università di Milano, Milano, Italy*
[71a]*INFN Sezione di Napoli, Italy*
[71b]*Dipartimento di Fisica, Università di Napoli, Napoli, Italy*
[72a]*INFN Sezione di Pavia, Italy*
[72b]*Dipartimento di Fisica, Università di Pavia, Pavia, Italy*
[73a]*INFN Sezione di Pisa, Italy*
[73b]*Dipartimento di Fisica E. Fermi, Università di Pisa, Pisa, Italy*
[74a]*INFN Sezione di Roma, Italy*
[74b]*Dipartimento di Fisica, Sapienza Università di Roma, Roma, Italy*
[75a]*INFN Sezione di Roma Tor Vergata, Italy*
[75b]*Dipartimento di Fisica, Università di Roma Tor Vergata, Roma, Italy*
[76a]*INFN Sezione di Roma Tre, Italy*
[76b]*Dipartimento di Matematica e Fisica, Università Roma Tre, Roma, Italy*
[77a]*INFN-TIFPA, Italy*
[77b]*Università degli Studi di Trento, Trento, Italy*
[78]*Department of Astro and Particle Physics, Universität Innsbruck, Innsbruck, Austria*
[79]*University of Iowa, Iowa City, Iowa, USA*
[80]*Department of Physics and Astronomy, Iowa State University, Ames, Iowa, USA*
[81a]*Departamento de Engenharia Elétrica, Universidade Federal de Juiz de Fora (UFJF), Juiz de Fora, Brazil*
[81b]*Universidade Federal do Rio De Janeiro COPPE/EE/IF, Rio de Janeiro, Brazil*
[81c]*Instituto de Física, Universidade de São Paulo, São Paulo, Brazil*
[81d]*Rio de Janeiro State University, Rio de Janeiro, Brazil*
[82]*KEK, High Energy Accelerator Research Organization, Tsukuba, Japan*
[83]*Graduate School of Science, Kobe University, Kobe, Japan*
[84a]*Faculty of Physics and Applied Computer Science, AGH University of Science and Technology, Krakow, Poland*
[84b]*Marian Smoluchowski Institute of Physics, Jagiellonian University, Krakow, Poland*
[85]*Institute of Nuclear Physics Polish Academy of Sciences, Krakow, Poland*
[86]*Faculty of Science, Kyoto University, Kyoto, Japan*
[87]*Kyoto University of Education, Kyoto, Japan*
[88]*Research Center for Advanced Particle Physics and Department of Physics, Kyushu University, Fukuoka, Japan*
[89]*Instituto de Física La Plata, Universidad Nacional de La Plata and CONICET, La Plata, Argentina*
[90]*Physics Department, Lancaster University, Lancaster, United Kingdom*
[91]*Oliver Lodge Laboratory, University of Liverpool, Liverpool, United Kingdom*
[92]*Department of Experimental Particle Physics, Jožef Stefan Institute and Department of Physics, University of Ljubljana, Ljubljana, Slovenia*
[93]*School of Physics and Astronomy, Queen Mary University of London, London, United Kingdom*
[94]*Department of Physics, Royal Holloway University of London, Egham, United Kingdom*
[95]*Department of Physics and Astronomy, University College London, London, United Kingdom*

[96]*Louisiana Tech University, Ruston, Louisiana, USA*
[97]*Fysiska Institutionen, Lunds Universitet, Lund, Sweden*
[98]*Departamento de Física Teorica C-15 and CIAFF, Universidad Autónoma de Madrid, Madrid, Spain*
[99]*Institut für Physik, Universität Mainz, Mainz, Germany*
[100]*School of Physics and Astronomy, University of Manchester, Manchester, United Kingdom*
[101]*CPPM, Aix-Marseille Université, CNRS/IN2P3, Marseille, France*
[102]*Department of Physics, University of Massachusetts, Amherst, Massachusetts, USA*
[103]*Department of Physics, McGill University, Montreal, Quebec, Canada*
[104]*School of Physics, University of Melbourne, Victoria, Australia*
[105]*Department of Physics, University of Michigan, Ann Arbor, Michigan, USA*
[106]*Department of Physics and Astronomy, Michigan State University, East Lansing, Michigan, USA*
[107]*Group of Particle Physics, University of Montreal, Montreal, Quebec, Canada*
[108]*Fakultät für Physik, Ludwig-Maximilians-Universität München, München, Germany*
[109]*Max-Planck-Institut für Physik (Werner-Heisenberg-Institut), München, Germany*
[110]*Graduate School of Science and Kobayashi-Maskawa Institute, Nagoya University, Nagoya, Japan*
[111]*Department of Physics and Astronomy, University of New Mexico, Albuquerque, New Mexico, USA*
[112]*Institute for Mathematics, Astrophysics and Particle Physics, Radboud University/Nikhef, Nijmegen, Netherlands*
[113]*Nikhef National Institute for Subatomic Physics and University of Amsterdam, Amsterdam, Netherlands*
[114]*Department of Physics, Northern Illinois University, DeKalb, Illinois, USA*
[115a]*New York University Abu Dhabi, Abu Dhabi, United Arab Emirates*
[115b]*United Arab Emirates University, Al Ain, United Arab Emirates*
[115c]*University of Sharjah, Sharjah, United Arab Emirates*
[116]*Department of Physics, New York University, New York, New York, USA*
[117]*Ochanomizu University, Otsuka, Bunkyo-ku, Tokyo, Japan*
[118]*Ohio State University, Columbus, Ohio, USA*
[119]*Homer L. Dodge Department of Physics and Astronomy, University of Oklahoma, Norman, Oklahoma, USA*
[120]*Department of Physics, Oklahoma State University, Stillwater, Oklahoma, USA*
[121]*Palacký University, Joint Laboratory of Optics, Olomouc, Czech Republic*
[122]*Institute for Fundamental Science, University of Oregon, Eugene, Oregon, USA*
[123]*Graduate School of Science, Osaka University, Osaka, Japan*
[124]*Department of Physics, University of Oslo, Oslo, Norway*
[125]*Department of Physics, Oxford University, Oxford, United Kingdom*
[126]*LPNHE, Sorbonne Université, Université Paris Cité, CNRS/IN2P3, Paris, France*
[127]*Department of Physics, University of Pennsylvania, Philadelphia, Pennsylvania, USA*
[128]*Department of Physics and Astronomy, University of Pittsburgh, Pittsburgh, Pennsylvania, USA*
[129a]*Laboratório de Instrumentação e Física Experimental de Partículas - LIP, Lisboa, Portugal*
[129b]*Departamento de Física, Faculdade de Ciências, Universidade de Lisboa, Lisboa, Portugal*
[129c]*Departamento de Física, Universidade de Coimbra, Coimbra, Portugal*
[129d]*Centro de Física Nuclear da Universidade de Lisboa, Lisboa, Portugal*
[129e]*Departamento de Física, Universidade do Minho, Braga, Portugal*
[129f]*Departamento de Física Teórica y del Cosmos, Universidad de Granada, Granada (Spain), Portugal*
[129g]*Instituto Superior Técnico, Universidade de Lisboa, Lisboa, Portugal*
[130]*Institute of Physics of the Czech Academy of Sciences, Prague, Czech Republic*
[131]*Czech Technical University in Prague, Prague, Czech Republic*
[132]*Charles University, Faculty of Mathematics and Physics, Prague, Czech Republic*
[133]*Particle Physics Department, Rutherford Appleton Laboratory, Didcot, United Kingdom*
[134]*IRFU, CEA, Université Paris-Saclay, Gif-sur-Yvette, France*
[135]*Santa Cruz Institute for Particle Physics, University of California Santa Cruz, Santa Cruz, California, USA*
[136a]*Departamento de Física, Pontificia Universidad Católica de Chile, Santiago, Chile*
[136b]*Millennium Institute for Subatomic Physics at High Energy Frontier (SAPHIR), Santiago, Chile*
[136c]*Instituto de Investigación Multidisciplinario en Ciencia y Tecnología, y Departamento de Física, Universidad de La Serena, Chile*
[136d]*Universidad Andres Bello, Department of Physics, Santiago, Chile*
[136e]*Instituto de Alta Investigación, Universidad de Tarapacá, Arica, Chile*
[136f]*Departamento de Física, Universidad Técnica Federico Santa María, Valparaíso, Chile*
[137]*Department of Physics, University of Washington, Seattle, Washington, USA*
[138]*Department of Physics and Astronomy, University of Sheffield, Sheffield, United Kingdom*
[139]*Department of Physics, Shinshu University, Nagano, Japan*
[140]*Department Physik, Universität Siegen, Siegen, Germany*
[141]*Department of Physics, Simon Fraser University, Burnaby, British Columbia, Canada*

[142]*SLAC National Accelerator Laboratory, Stanford, California, USA*
[143]*Department of Physics, Royal Institute of Technology, Stockholm, Sweden*
[144]*Department of Physics and Astronomy, Stony Brook University, Stony Brook, New York, USA*
[145]*Department of Physics and Astronomy, University of Sussex, Brighton, United Kingdom*
[146]*School of Physics, University of Sydney, Sydney, Australia*
[147]*Institute of Physics, Academia Sinica, Taipei, Taiwan*
[148a]*E. Andronikashvili Institute of Physics, Iv. Javakhishvili Tbilisi State University, Tbilisi, Georgia*
[148b]*High Energy Physics Institute, Tbilisi State University, Tbilisi, Georgia*
[148c]*University of Georgia, Tbilisi, Georgia*
[149]*Department of Physics, Technion, Israel Institute of Technology, Haifa, Israel*
[150]*Raymond and Beverly Sackler School of Physics and Astronomy, Tel Aviv University, Tel Aviv, Israel*
[151]*Department of Physics, Aristotle University of Thessaloniki, Thessaloniki, Greece*
[152]*International Center for Elementary Particle Physics and Department of Physics, University of Tokyo, Tokyo, Japan*
[153]*Department of Physics, Tokyo Institute of Technology, Tokyo, Japan*
[154]*Department of Physics, University of Toronto, Toronto, Ontario, Canada*
[155a]*TRIUMF, Vancouver, British Columbia, Canada*
[155b]*Department of Physics and Astronomy, York University, Toronto, Ontario, Canada*
[156]*Division of Physics and Tomonaga Center for the History of the Universe, Faculty of Pure and Applied Sciences, University of Tsukuba, Tsukuba, Japan*
[157]*Department of Physics and Astronomy, Tufts University, Medford, Massachusetts, USA*
[158]*Department of Physics and Astronomy, University of California Irvine, Irvine, California, USA*
[159]*Department of Physics and Astronomy, University of Uppsala, Uppsala, Sweden*
[160]*Department of Physics, University of Illinois, Urbana, Illinois, USA*
[161]*Instituto de Física Corpuscular (IFIC), Centro Mixto Universidad de Valencia - CSIC, Valencia, Spain*
[162]*Department of Physics, University of British Columbia, Vancouver, British Columbia, Canada*
[163]*Department of Physics and Astronomy, University of Victoria, Victoria, British Columbia, Canada*
[164]*Fakultät für Physik und Astronomie, Julius-Maximilians-Universität Würzburg, Würzburg, Germany*
[165]*Department of Physics, University of Warwick, Coventry, United Kingdom*
[166]*Waseda University, Tokyo, Japan*
[167]*Department of Particle Physics and Astrophysics, Weizmann Institute of Science, Rehovot, Israel*
[168]*Department of Physics, University of Wisconsin, Madison, Wisconsin, USA*
[169]*Fakultät für Mathematik und Naturwissenschaften, Fachgruppe Physik, Bergische Universität Wuppertal, Wuppertal, Germany*
[170]*Department of Physics, Yale University, New Haven, Connecticut, USA*

[a]Also at Department of Physics, King's College London, London, United Kingdom.
[b]Also at Institute of Physics, Azerbaijan Academy of Sciences, Baku, Azerbaijan.
[c]Also at Lawrence Livermore National Laboratory, Livermore, California, USA.
[d]Also at TRIUMF, Vancouver, British Columbia, Canada.
[e]Also at Department of Physics, University of Thessaly, Volos, Greece.
[f]Also at Physics Department, An-Najah National University, Nablus, Palestine.
[g]Also at Department of Physics, University of Fribourg, Fribourg, Switzerland.
[h]Also at Department of Physics and Astronomy, University of Louisville, Louisville, Kentucky, USA.
[i]Deceased.
[j]Also at Department of Physics, Westmont College, Santa Barbara, California, USA.
[k]Also at Departament de Fisica de la Universitat Autonoma de Barcelona, Barcelona, Spain.
[l]Also affiliated with an institute covered by a cooperation agreement with CERN.
[m]Also at The Collaborative Innovation Center of Quantum Matter (CICQM), Beijing, China.
[n]Also at Department of Physics, Ben Gurion University of the Negev, Beer Sheva, Israel.
[o]Also at Università di Napoli Parthenope, Napoli, Italy.
[p]Also at Institute of Particle Physics (IPP), Victoria, British Columbia, Canada.
[q]Also at Bruno Kessler Foundation, Trento, Italy.
[r]Also at Borough of Manhattan Community College, City University of New York, New York, New York, USA.
[s]Also at Department of Physics, University of Colorado Boulder, Boulder, Colorado, USA.
[t]Also at Department of Financial and Management Engineering, University of the Aegean, Chios, Greece.
[u]Also at Centro Studi e Ricerche Enrico Fermi, Rome, Italy.
[v]Also at Department of Physics, California State University, East Bay, California, USA.
[w]Also at Institucio Catalana de Recerca i Estudis Avancats, ICREA, Barcelona, Spain.
[x]Also at University of Chinese Academy of Sciences (UCAS), Beijing, China.
[y]Also at Physics Department, Yeditepe University, Istanbul, Türkiye.
[z]Also at Institute of Theoretical Physics, Ilia State University, Tbilisi, Georgia.

[aa]Also at CERN, Geneva, Switzerland.
[ab]Also at Hellenic Open University, Patras, Greece.
[ac]Also at Center for High Energy Physics, Peking University, China.
[ad]Also at The City College of New York, New York, New York, USA.
[ae]Also at Department of Physics, California State University, Sacramento, California, USA.
[af]Also at Département de Physique Nucléaire et Corpusculaire, Université de Genève, Genève, Switzerland.
[ag]Also at Institut für Experimentalphysik, Universität Hamburg, Hamburg, Germany.
[ah]Also at Department of Physics and Astronomy, Michigan State University, East Lansing, Michigan, USA.